5-6-2020

Zebrafish Eye Development: Rac and the Creepy Crawlers of the Eye

Zvi Murry
murr7085@bears.unco.edu

UNIVERSITY OF NORTHERN COLORADO

Greeley, Colorado

The Graduate School

ZEBRAFISH EYE DEVELOPMENT: RAC AND THE CREEPY CRAWLERS OF THE EYE

A Thesis Submitted in Partial Fulfillment
of the requirements for the Degree of
Master of Science

Zvi Cherokee Murry

College of Natural and Health Sciences
School of Biological Sciences

May 2020

This Thesis by: Zvi Cherokee Murry

Entitled: *Zebrafish Eye Development: Rac and the Creepy Crawlers of the Eye*

has been approved as meeting the requirement for the Degree of Master of Science in College of Natural and Health Sciences in School of Biological Sciences, Program of Biological Sciences.

Accepted by the Thesis Committee:

_____
Andrea E. James, Ph.D., Committee Chair

_____
Patrick D. Burns, Ph.D., Committee Member

_____
Emily A. Holt, Ph.D., Committee Member

Accepted by the Graduate School

_____
Cindy Wesley
Interim Associate Provost and Dean
The Graduate School and International Admissions

ABSTRACT

Murry, Zvi. *Zebrafish Eye Development: Rac and the Creepy Crawlers of the Eye.* Unpublished Master of Science thesis, University of Northern Colorado, 2020.

During vertebrate eye development the optic vesicles protrude from either side of the brain and form the optic cups. As an optic cup starts to surround the lens a groove on the ventral side of the eye forms, known as the choroid fissure (CF). Normally, the CF will close around the optic nerve and hyaloid vasculature. If this process does not occur properly it results in a keyhole opening in the eye known as coloboma. This results in blindness and affects nearly 1 in 4-5,000 births. Zebrafish were utilized as a model for eye development to study CF closure (CFC) as they utilize similar gene expression and cellular signaling. Previously, a transient β-catenin/actin fusion seam within the fusing CF was observed indicating the formation of cell-to-cell contacts. Rac, a small G-protein, regulates actin cytoskeleton reorganization and formation of lamellipodia required for cell-to-cell adhesion. These lamellipodia increase interactions between cells increasing contacts that could form adherens junctions. *I hypothesized Rac would be expressed prior to CFC and dissipate upon CFC completion, similar to adhesion proteins.* To determine Rac's localization, embryos were cryosectioned at 47 and 49-hours post-fertilization (hpf) and Rac immunofluorescence was observed. These data demonstrated Rac is present within the CF edges at 47 hpf and dissipates the CF fusion seam as CFC progresses in wildtypes embryos around 49 hpf. Quantification of these data further demonstrated a progressive fusion event that initiates in the central section of the CF an

moves bidirectionally towards the proximal and distal edges, emulating a zipper-like fashion. *in vivo* analysis of *Rx3:*GFP embryos (neuroretina labeled) identified a subpopulation of cells that are present within the CF at 24 hpf. This population of cells appear highly protrusive and "reach" in multiple directions. Further analysis of Rac embryos identified these "reaching cells" as Rac positive. *in vivo* analysis of this cell population revealed that seven identified categories of reaching cells can be divided into three stages of CFC. Rac is also required for reaching cells. When observing the Rac-DN embryo no reaching cells were ever observed, regardless of heat-shocking time. The Rac-DN embryos showed an abnormal optic cup angle and unusual cuboidal cells shapes (early heat-shock). In later heat-shocked times the abnormal angle and unusual cell shapes were resolved, however, there were unusual division patterns that were observed. Further investigation is ongoing to identify the role of Rac in this cell population and the role of "reaching cells" during zebrafish eye development.

ACKNOWLEDGEMENTS

I wish to express my sincere appreciation to my PI, Dr. Andrea James, who encouraged me to push myself even when the road got tough. Without her help and belief in me the goal of this project would not have been achieved.

I would like to recognize the invaluable assistance of Patrick Burns and Emily Holt, my committee members, who truly helped turn this thesis into an understandable story to share.

I wish to thank all the members of the James Lab. I have made lifelong friendships with all of you and this milestone of a completed project was possible because of the support you all unwaveringly gave. I would especially like to thank Carmen Rodriguez and Brandon Selz, without you both, my second aim would have never been completed.

I wish to pay special regards to the employees of the Animal Facility who aided in caring for my fish when I could not. Especially, Laura Martin, who believed in me every single day and brought a smile to my face always.

I would also like to show my deep appreciation to Chad Wangeline and Casey Rodgers who taught me how to take the beautiful images presented in this these.

A special thanks to Cindy Budde and Elizabeth Buller who turned the bad days around and will always be a priceless contribution to student success.

The physical and technical contribution of ‘The Knights Templar Grant’ and ‘UNCO Graduate School’ is truly appreciated. Without their support and funding, this project could not have reached its goal.

A special thank you to the Gross lab for their generous gifts of zebrafish used in this thesis.

I also wish to acknowledge the support and great love of my family, my sister, Tchuen Yi; my mother, Francie; my father, Brandon; my boyfriend; Taylor, and my best friends; Prim and Teal. They kept me going through love, laughs, warm hugs, long walks, and good food. This work would not have been possible without you all. I love you all so much!

TABLE OF CONTENTS

CHAPTER

I. INTRODUCTION 1
Introduction to the Study
Why Use Zebrafish
Thesis Organization
Vertebrate Eye Development
Stage 1: Specification Within the Forebrain to Distinguish the Eye Field
Stage 2: Genetic and Morphogenic Creation of the Optic Vesical
Stage 3: Specification of the Neural Retinal and Retinal Pigment Epithelium
Stage 4: Lamination of Retinal Cell Types and Retinal Pigment Epithelium
Adhesion in Vertebrate Eye Development
Summary

II. METHODOLOGY 21
Fish Husbandry
Embryo Collection
Cryosections
Immunofluorescence
Confocal Imaging – Fixed Imaging
Intensity Measurements
Heat-shock of Embryos for *in vivo* Imaging
Embryo Screening
in vivo Imaging Preparation
Confocal Imaging - *in vivo*
Post Confocal Imaging - *in vivo*
Data Analysis of Reaching Cells
Rac-GEF Inhibitor

III. RESULTS 31
Rac Localizes at Edges of Choroid Fissure Prior to Fusion Markers
Rac is Not Localized with Choroid Fissure During Fission Events
Quantification of Rac Fluorescence Intensity at 47/49 hours post-fertilization
Reaching Cells Are Present in Fixed Tissue at 49 hours post-fertilization
Spaciotemporal Appearance of the Reaching Cells in an *Rx3*:GFP Background
Cellular Dynamics of the Reaching Cells in an *Rx3*:GFP Background
Reaching Cells Not Observed in A Dominant Negative Rac Zebrafish
Reaching Cells/Rac Activity are Required for Proper Choroid Fissure Closure

IV. CONCLUSIONS 44

REFERENCES 53

APPENDIX

A. Institutional Animal Care and Use Committee Approval.....70

LIST OF FIGURES

FIGURE

1. Heavy Seam of Rac Localization at CF in Proximal Central and Distal Central Sections of the Eye at 47 hpf in Wildtype. 32

2. Rac Localization No Longer Present as a Seam in Either Proximal Central or Distal Central Sections of the Eye at 49 hpf in Wildtype. 33

3. Photographic Illustration of Where Intensity Measurements Were Taken. 34

4. Box Plots of Rac Localization Intensity Ratio at 47 hpf Compared to 49 hpf in 5 Positions of the Eye. 35

5. Reaching Cells in Fixed Tissue at 49 hpf Contact Retina to Retina and up to the Lens. 36

6. Reaching Cells Progressively Move Towards the CF as Development Proceeds. 38

7. Dynamics of the Reaching Cells Categorizing Based on Cellular Shapes and Dynamics Displayed Along with Timeframes Observed *in vivo*. 40

8. Effects of Early and Late HS Induction of Rac-DN Expression. 42

9. Reaching Cells/Rac Activity are Required for Proper CFC. 43

CHAPTER I

INTRODUCTION

Introduction to the Study

Vision impairment substantially impacts quality of human life (1,2). Vision impairment is commonly associated with other health concerns. For example, often people who have vision impairments also have hearing impairments, epilepsy, intellectual disabilities, cerebral palsy, autism spectrum disorder, and non-24-hour sleep-wake disorder (3-6). Maintaining independence as an adult with vision impairment can be challenging for reasons such as: employment adversity, incredulous medical costs, which create financial burdens, and conditions that makes providing for a family extremely difficult (7). According to the U.S. Centers for Disease Control and Prevention (CDC), vision problems are the single most prevalent disabling condition among American children. The CDC reports that approximately 780 U.S. babies are born with eye abnormalities each year. By the time children reach school, a quarter of American children suffer from a vision problem. Therefore, almost 12.5 million school-aged kids may be unable to see the teaching materials at a far-point (8). Considering 80% of human sensory connection is through our eyes, not having this ability can cause tremendous brain development issues, social issues, and developmental delays later in life (9,10).

Research into the development of the vertebrate eye is essential because it will increase our understanding of how some of these problems occur and could lead to possible treatments. One ocular disease that has a tremendous gap in scientific and

clinical knowledge is termed coloboma. This is an ocular disorder that leaves a keyhole appearance at the dorsal region of the eye (11,12). Unfortunately, the cellular and molecular dynamics that lead to coloboma is relatively unknown. However, it has been proposed that this disorder is linked to the choroid fissure (CF) failing to fuse and adhere properly (13). Coloboma affects about 1 in 10,000 human births, resulting in blindness (12,14).

Previous studies have demonstrated a consistency in gene expression, localization of gene expression patterns within tissues, required tissue shapes, and transcription factors in multiple animals that is required for normal eye development. For example, in early eye development, the transcription factor *Pax* is key in initiating primitive eye fields and is required for proper eye development (15,16). In addition, the transcription factor *Vax* is expressed in the developing forebrain and optic nerve and is essential for normal development of these structures (17). In later stages, *lamb1* and *lamc1*, extracellular matrix proteins, are required for proper optic cup formation and retina containment (18,19). In all these cases, there is a resulting coloboma due to the lack of proper choroid fissure closure (CFC), if these factors are not expressed appropriately. Later fusion stages of eye development that focus on cellular adhesion had not, however, been characterized in as great of detail.

My overarching research goal was to characterize a group of cells I termed "reaching cells," as I observed them making attachments between multiple tissues. My research began with identifying markers for their presence and characterizing aspects of their presence and movement dynamics in the developing zebrafish eye.

With this research, I had two specific aims with associated questions and hypotheses:

A1 I sought to characterize the appearance and dynamics of reaching cells in a wild-type *Rx3*:GFP zebrafish.

Q1a At what developmental time point do the reaching cells first appear during eye development?

Q1b What connections do the reaching cells make in the distal section of the eye?

Q1c Does this cell population exhibit the same characteristics, such as placement and shape, regardless of developmental time point?

H1 I hypothesized the reaching cells would be present during initiation until completion of CFC, arriving at the eye 24 hours post fertilization (hpf), making the same, if not new connections, to various tissue types in the eye, always displaying the same dynamics regardless of location or developmental time point.

A2 I sought to determine if molecular regulation is required for the spatiotemporal dynamics observed in *Rx3*:GFP reaching cells by utilizing a *hs70l:*Gal4*; UAS:*Rac-DN temporal expression transgenic fish to over-express a dominant negative version of Rac.

H2 I hypothesized that reaching cells would be present during CF closure; however, I predicted that there would be fewer reaching cells within the eye field, in the CF, and the few that are there would not make the same connections as seen in the wild-type (WT).

Why Use Zebrafish

Danio rerio more commonly known as zebrafish are small freshwater fish that belong to the minnow family. Zebrafish have become very popular in the last twenty years due to an increase of use in the scientific community as a vertebrate model organism (20,21). Zebrafish are an ideal model organism to explore eye development and cell populations because embryo development occurs outside the mother, the embryos are transparent, the adults produce many young, the embryos and adults are easy to maintain,

the zebrafish whole genome has been sequenced, the model has similar genetic structure and organ structure compared to humans, and mutant and transgenic strains, are readily available (22).

Thesis Organization

In this thesis, I followed the four-chapter format approved by the School of Biological Sciences. I began with a general introduction to the importance of studying eye development, why zebrafish were chosen as my model organism, and outlined what this thesis sought to address with two aims. I then included the primary literature related to vertebrate ocular development, coloboma, and morphogenetic movements during eye tissue formation. In addition, I discussed the molecular regulations, cell adhesion, and migration required for these morphogenetic movements. In Chapter II, I presented the methodology used to achieve the two thesis aims. Chapter III is a presentation of the results of the experiments performed. Chapter IV concludes with a discussion of my findings and suggestions for future work. Appendix A contains the Institutional Animal Care and Use Committee approval for this research.

Vertebrate Eye Development

Vertebrate eye development is an intricate and involved process. Many cells and tissue layers migrate, interact, and communicate as the developmental process of the eye occurs. These processes can be regulated by intrinsic (transcription factors) or extrinsic (growth factors) factors and helps to specify what tissue will become the eye and what tissue will become the brain (fully reviewed in 23). Vertebrate eye development had been previously described in four distinct stages: 1) specification within the forebrain to

distinguish the eye field; 2) genetic and morphogenic creation of the optic vesicle; 3) specification of the neural retina and retina pigment epithelium (RPE), and 4) lamination of the seven retinal cell types and RPE (23). This review will discuss the mutation analysis of each of these phases which have collectively demonstrated all four stages are required for proper vertebrate ocular development.

Stage 1: Specification Within the Forebrain to Distinguish the Eye Field

During stage 1 of vertebrate eye development many signaling pathways are utilized to distinguish and specify the eye field. Previously it was established that Wnt8 is required for proper eye field formation out of the forebrain (24). This signaling gradient is required to create anterior to posterior directionality within neural fated tissue in both fish and frogs (25,26). Zebrafish Wnt mutants present with cyclopia, if eyes are present at all (27). This outcome is thought to be a result of a reduced telencephalon, which is the source of the eye field (27). Mutations within the Wnt signaling pathway present with multiple ocular malformation and defects in both retina and lens indicating a broader role in eye development (28,29).

Otx2 also plays a large role in stage 1 of eye development. Otx2 is required for the forebrain to specify what tissue will become the eye field (30). This will then induce transcription factor expression to help develop the eye field (30). Eye field transcription factors, expressed in the anterior neural plate, such as Rx, Pax6, Six3/6, Lhx2, Optx2, and Tbx genes have been studied in detail (fully reviewed in 30,31). Loss of function of these transcription factors (i.e., Rx (32); Pax6 (33); Six3 (34,35); and Lhx2 (36)) lead to phenotypes previously observed in loss of Wnt, such as no eyes or irregular eyes (27-29). Overexpression of these transcription (Rx (37); Pax6 (33); Six3(35,36)) factors can

induce an ectopic eye. Otx2 has not been shown to directly bind and induce expression of these transcription factors, indicating there may be a mediating transcription factor that has yet to be determined (30).

Transcription factors can lead to controlled segregation behavior of retinal progenitor cells (RPCs). Within the eye field, Optx2 (30,31) and Rx are regulators of proliferation (39). Other work has shown that Rx may act in suppressing a canonical Wnt pathway, thus preventing the induction of anterior-posterior neural plate fate (39). This suppression promotes non-canonical Wnt signaling that in turn controls morphogenetic movements of ocular cells (40). RPCs first make a movement to the midline and then move outward into the evaginating optic vesical (OV) (41) which initiates the transition into the next stage. Collectively these studies demonstrate how multiple model organisms reveal intrinsic factors, such as expression of transcription factors that control segregation behavior of RPCs (24-33,35-39,41-48).

Upon transcriptional differentiation of the eye field, two independent eye fields begin to emerge. Sonic hedgehog signaling (Shh) is essential for establishing this midline (44). In a Shh mutant, Pax 6 is overexpressed indicating Shh plays a role in suppressing Pax6 expression in the center/midline of the neural tube. These mutants also fail to establish two identical eye fields resulting in a single eye located in the midline and holoprosencephaly (enlarged brain) (44). Shh mutants further fail to upregulate Pax2, which is required for proliferation of the eye field, and Six3, used to repress Wnt (36,44-46). If these events are not completed in the appropriate order, timing, and stage, it will disrupt events later in eye development. In some cases, the following stages can still

begin even if an earlier stage is disrupted, just as observed in the Shh example above (36,43-46).

Stage 2: Genetic and Morphogenic Creation of the Optic Vesicle

During stage 2, two specified eye fields proceed through a series of morphological and molecular signaling creating the OV from the brain and the lens from the skin (47,48). After the division of the eye field the OV is formed. OV evagination occurs on both sides of the ventral forebrain during the final stages of neural tube formation and is dependent on Shh signaling (49-54). Changes in cell shape and location are required to drive this evagination process. In mice, the cellular shape of the OV cells change dramatically accompanied by temporary basal lamina composition (55). In zebrafish, these eye cells have extensive movement that is essential for organogenesis of the OV. Fish retina progenitor cells show a direct movement toward the midline of the body followed by an outward turn into the evaginating OV (41). In chicken and mouse models, these movements are still relatively unknown.

Retinal homeodomain transcription factor, Rx, mediates some of these cellular behaviors at a molecular level. In multiple animal models, it has shown that Rx can cause only one eye to form or no eyes at all to develop, indicating the importance of Rx genes in early development (56-59). Rx3 null mutant zebrafish have shown that OV evagination is disrupted specifically in the outward direction of the cell movements that are key for evagination (41,56,60,61). In mice, embryos chimeric for $Rx3^{+/+}$vs $Rx3^{-/-}$ demonstrated that $Rx3^{-/-}$ cells are excluded from the OV domains (62), indicating a role for adhesion during this migration process. Rx genes may further play a role in regulation of expression of adhesion molecules. Rx3 contains a binding site for the Nlcam locus, an Ig-

dominate cell adhesion molecule (63). With reduced Rx3 mRNA expression Nlcam has an expanded mRNA expression pattern (63). This pattern indicates that as Rx3 is required for reducing Nlcam mRNA expression, it is ectopically upregulated in the eye field (63). In addition, Rx3 $^{-/-}$ embryos present with a smaller eye and cells displayed increased convergence at the midline (63). These results indicate Nlcam expression and Rx3 may be necessary to enable retinal progenitor cells to move away from the midline of the eye field and outward to play a role to the evaginating OV (63). Overall, stage 2 encompasses cell signaling that leads to changes in cell shape and changes in cell behaviors. Furthermore, Rx expression is involved extensively in regulating cell movements integral for OV evagination.

Stage 3: Specification of the Neural Retinal and Retina Pigment Epithelium

After the OV has successfully evaginated from the central mid-line, the OV will transition into a double-layered structure known as the optic cup (OC), while concurrently the invagination and migration of the ectoderm forms the lens vesicle (LV) (40). The enveloping of the lens is initiated superficially as well as anteriorly, resulting in the OC needing to close on the posterior, or bottom, of what will become the eye (40). The following series of cell signaling events has been associated with this process.

As the optic vesicle extends and interacts with the ectoderm, bone morphogenetic protein (BMP) signaling is utilized to begin the formation of the lens placode (LP) (64). In chicken, BMPs are expressed in the ectoderm at the anterior portion of the neural plate (65) and the region correlates with where lens progenitor cells initiate (66). In mice, BMP is present at the head surface ectoderm during the time of LP induction although this gradually decreases in the LP and eventually dissipates from the LV (67-70).

Fibroblast Growth Factor (FGF) signaling is also a key player in this stage. FGF signals help with development and morphogenesis of the eye, especially in retina and periocular mesenchyme (POM) (71-77). FGF is known to play a role in organogenesis to maintain progenitor cells and mediate their proliferation, help with differentiation, survival of these cells, and patterning to help cells proceed to the correct locations (78-81). While this signaling is thought to be required for proper OV and LP specification (82), recent evidence has demonstrated that the lack of lens development in later stages still allows retinal differentiation and lamination to occur (83).

During OC and lens formation, the distal portion of the OV will make a connection with the overlying surface ectoderm (40,84). When this connection occurs, the specification of the lens ectoderm (lens pit) is initiated. This interaction will lead to invagination of the LP and distal OV will form a bilayer OC (85). The lens vesicle eventually separates from the surface ectoderm and differentiates into the lens. While lens vesicle tissue movements have been described, the mechanical forces behind the morphogenesis of invagination are just beginning to be understood.

One area of study is the potential of force and tension required during ocular field morphogenesis. In chicken models, it has been shown that invagination is a calcium-dependent process, but the force comes from the apical bands of microfilaments that are located in the retina cells that contract to enable OC formation (84). In *medaka*, studies were done on a gene that encodes for a transmembrane protein that when mutant presents similar orofacial clefting syndrome with eye abnormalities (40,86). There were several morphogenesis defects such as improper invagination of the OC (40,86). Only a partial OC was formed and integrin receptors in the basal surface of the retina appeared reduced

(40). It was proposed that reduced tension and a change in cellular shape of the RPCs led to the abnormalities (40).

Filopodia may provide the cellular structure providing the mechanical force necessary for invagination of the OC. As invagination of the OV and evagination of the LP are synchronized both tissues are in juxtaposition (84). Research revealed that basal filopodia, that mostly originate from the lens ectoderm, rapidly tether the forming lens and retina to complete invagination of the LP (85). Production of these filipodia require expression of both Rho GTPase, Cdc42, and the effector of IRSp53 (85). Lack of either of these leads to a defect in the LP invagination (85). Further studies are needed to identify the molecular regulation that regulates the morphogenic process.

As the OC and lens placode are in tight juxtaposition while morphogenesis is occurring it is possible the process of invagination is dependent upon tissue-to-tissue interactions. When pre-placodal ectoderm is ablated from the OV, the distal OV invagination is disrupted, although the retina continues to specify (87), indicating morphogenic movements are regulated separately rather than by differentiation. Nevertheless, if surface ectoderm ablation occurs at the LP stage, the OC forms correctly without a properly developed lens (87,88). These experiments show that invagination requires specific and precisely timed interactions between tissues for proper ocular development.

During the latter timeframe of stage 3, the OV begins to differentiate a bilayer structure with the inner layer developing into the neural retina (NR) and the outer layer developing into the retinal pigmented epithelium (RPE) (89). NR is derived from the distal-ventral portion of the OV, but, the RPE is derived from the dorsal region (90,91).

During stages 1 and through early stage 2, the neuroepithelium is bipotential and thus the presumptive NR is competent to develop into the RPE (92-98). The presumptive RPE can then develop into the NR (99-101). In chicken, the dorsal-ventral portions of the OV have distinct developmental potency. When researchers removed the dorsal OV, the anterior-ventral domains regenerated the retina and the RPE (102). However, the dorsal portion can only develop into an RPE-like vesicle that did not invaginate (102). Thus, the anterior-ventral domain of the OV may be the driving force of morphogenesis of proper tissue specification of the ocular field (102).

The earliest known patterning gene expressed in the ocular field is the LIM homeobox transcription factor Lhx2 (30,102). In Lhx2 mouse mutants, expression of the ocular field transcription factors initiated normally but eye development arrested at the OV stage (34,102). The lens failed to form since the expression of the OV regional patterning markers were expanded (34,103). Overall, these genes were able to be categorized into two different segments: genes such as Mitf, Chx10, Vsx2 and Tbx5 are never initiated, while the expression of Pax2, Vax2, and Rx are initiated but not maintained (103). Therefore, we know Lhx2 is required in genesis of OV specification into the NR and RPE to then regulate the OC formation.

The RPE is responsible for multiple developmental aspects of the eye. The RPE regulates differentiation of photoreceptors, proper lamination of the retina, and most importantly the growth of the eye (40,104,105). Disruption of RPE specific genes results in microphthalmia, RPE-to-retina trans-differentiation and coloboma during eye development (106-111).

Intrinsic factors are known to regulate aspects of early RPE development. In zebrafish, lack of Rx3 expression can interfere with RPE development (112). It was also proposed that Rx induces competence on the presumptive RPE to respond to inducing signals from the mesenchyme (113). After these movements have been completed correctly stage 3 is now complete. It is important to remember that even if these movements do not happen successfully, progression into stage 4 is still a possibility in some cases.

Stage 4: Lamination of the Retinal Cell Types and Retinal Pigment Epithelium

The neural retina in its differentiated laminated state is generally referred to by the anatomical name, retina. The retina is part of the central nervous system that is responsible for protecting, processing, and sending visual information to the brain (114). To maintain and fulfill this role requires the retina be highly organized. Since vertebrate's retina is inverted, light must pass through the whole tissue before photoreceptors receive a signal (115) and a neural signal is sent through the optic nerve to the brain (116). When light is passed through the retinal tissue it is imperative to avoid light scatter. Studies have shown that due to the way the retina is organized, it helps to reduce or prevent light scatter by limiting the number of neurons receiving light signals (117). To solve limitations such as this and maintain signal processing (color, depth, motion) in such a small area (118,119), the neural retinal is arranged into distinct layers with respect to their function (114,120). This is known as retinal lamination (114,120).

Much like cells of the cerebral cortex, retinal cells show a histogenetic arrangement. Retinal ganglion cells (RGC) that are developed early on occupy the inner-

most retinal layer, while photoreceptors, that appear later, occupy the outermost retinal layer in vertebrates (74,121). Different retinal cell types have different birthdays. However, with seven different cell types and RPE, some cells' birthdays can overlap. Eventually, the seven presumptive cell types and RPE align in an apical to basal orientation with nuclei towards the inner retina having early birthdays and nuclei at the outer retina having later birthdays (122). Fate mapping studies done in zebrafish showed sister cells are born at the same time, however, migrate to different locations to set-up appropriate lamination of the retina (123). Late-born RGC migrate through a layer of early born amacrine cells to reach the appropriate RGC layer (122). There is also a period where postmitotic cell intermingle before they are sorted into the correct retinal layer (124).

One question these studies fail to address is whether these behaviors occur due to cell-to-cell interactions, response to environment, developmental checkpoints, or signaling gradients that are required. Interestingly, lamination will be preserved even in the absence of specific cell type (125-128), supporting a mechanism of organization for the retinal layers that cannot simply be determined by timing alone (126). Direct interactions between cell types are likely to be involved in the normal retina lamination process that aligns apical to basal (124,129). The involvement of cell-to-cell interactions is a key part of rosette formation in retinoblastoma (130) and retinal dysplasia's where cell adhesion molecules, such as N-cadherin, functionality is compromised (131), demonstrating a role for adhesion during retinal development.

Stage 4 is the culmination of a progressive process. In the zebrafish at 24 hours post-fertilization (hpf), the retina is pseudostratified epithelium comprised of about 2,000

progenitor cells that stretch from the apical to basal surface (123). From 48 hpf-72 hpf the progenitor cells will divide repeatedly, giving rise to a fully laminated retina containing the postmitotic neurons and glia of the major cells of the eye (123). As neuroepithelia cells becomes differentiated, the retina becomes stratified and the seven main neurons (retinal ganglion cells, the cone and rod photoreceptors, bipolar cells, amacrine, and horizontal cells, Müller glia) occupy this space surrounded by RPE (132,133). Upon completion of lamination, stage 4 is complete.

Adhesion in Vertebrate Eye Development

As these four stages occur, the eye field is developed, and the vertebrate eye adhesion molecules help shape and construct the eye into the proper structure and functionality by regulating cellular adhesive properties. As discussed above, it is vital that the different cell types undergo specific morphogenesis so the tissue will develop appropriately in the correct space and at the right time.

There are four major categories of cell adhesion molecules. One way to classify adhesion molecules is on their calcium-dependency or lack thereof, the former which include immunoglobulins, such as Nlcam, and cadherins, while the latter includes calcium-independent selectins and integrins (134). This distinction can further be associated with how these molecules will interact between two cells, either homophilic versus heterophilic (135,136). Both calcium-independent and dependent molecules have been observed during the spatiotemporal development of the eye tissues (19,137,138).

During stage 1 and 2, RPCs move to the midline of the embryo and then change directions to migrate to the evaginating optic vesicle (40,41). Forebrain cells that are in proximity to the midline come together rapidly and then are maintained at the midline

(41,43,63). Rx3 is a major transcription factor in differentiating these cell behavior changes likely through regulation of an Ig-domain protein, Nlcam (63). In the absence of Rx3 ectopic expression of Nlcam, enhanced convergence of these cells indicating these cells form part of the guidance directed migration patterning to the midline of the precursor forebrain cells (63). Thus, expression levels of Nlcam regulate migratory properties of the retinal progenitor cells (63). There is also evidence to suggest that the two phases of OV morphogenesis (slow convergence and outward-directed migration) are under different genetic control although that mechanism has yet to be determined (63). If true, it means that the OV formation during stage 1 and 2 is heavily dependent on Rx3 and Nlcam and is under a different mechanistic control.

Epithelial-cadherin (E-cadherin) is believed to be essential during eye development, in multiple organisms (139,140,141). Zebrafish morpholino knockdowns showed that anterior head structures of fish and lateral eye field is present but extremely unorganized (142). Other experiments have examined E-cadherin expression in the developing ventral midline signaling (pax2) using *cyclops* mutant embryos (142,143). *Cyclops'* mutants present with lack of or reduced E-cadherin mRNA expression compared to the wild-type (WT) (142). These mutants furthermore have a reduced optic stalk and the development of the retinal tissue expands along the ventral margin of the diencephalon, resulting in a single fused eye field (143). Taken together these data demonstrate adhesion molecules are an essential component during early stages of development to maintain normalcy. Unfortunately, in many model organisms, embryos lacking adhesion molecules to make these cell-to-cell connections do not survive past gastrulation (139-141). During these early stages of eye development few data have been

collected. A few studies in zebrafish can bridge this gap (136,144), since the embryos survive past gastrulation, a trait, many other model organisms fail to do (139-141).

During stage 3, specification of the neural retina and RPE, cadherin molecules remain essential as seen in stages 1 and 2. RPE cells lack E-cadherin but express Neural-cadherin (N-cadherin) at stage 2 in cell culture (145). *in vitro* analysis showed that RPE cells that underwent time-dependent changes were similar to epithelial cells that express E-cadherin. The cadherin gradually developed a zonular distribution of detergent-resistant protein that co-localized with forming a spherical actin bundle that then polarized to an apical RPE membrane (145), which is a classic sign of an adherent tissue. The E-cadherin RPE adhesion molecules did not develop such developmental patterns as observed with N-cadherin, but interestingly enough, the same cell-to-cell contact sites complements adhesion proteins that were expressed and observed (145). Although these RPE cells were expressing E-cadherin, there was an absence of epithelial properties. Specifically, there was a reduction of adherens junction's protein expression, which reduced actin colocalization as typically observed in the WT (145). Surprisingly, the RPE was not lacking N-cadherin, α-catenin, and β-catenin protein expression similar to that observed in epithelial cells (145).

As eye development reaches stage 3, the OV has invaginated to form a double-layered OC and the inner layer is composed of prospective neural retina cells and the outer layer known as the RPE, leading to the CF, a transient structure on the ventral portion of the eye (71,86,146,147). As stage 3 comes to a close, a vital step in eye development occurs, CFC. This transient structure is at the back/proximal portion of the eye. This structure is the location for entry of vasculature into the eye and exit of retinal

ganglion cells from the eye. When the CF fails to close, the consequence is a defect in morphogenesis of the eye called a coloboma (13). This is one of the most common eye congenital defects and can significantly impact one's vision, occurring in 1 out of 4-5,000 live births and causes 3-11% of childhood blindness (12,14,148-150).

This fusion process is complex and takes many adhesion molecules and regulators to ensure that proper eye field formation occurs. Rac is a key regulator in this process, promoting membrane ruffling and F-actin to spread to accomplish cell-to-cell contact (151). It has been shown in a previous study that the CF closes in three steps (152). Step 1 is tissue growth and OC morphogenesis (20-31 hfp) to bring the two pieces of the CF closer in proximity to one another in order for adhesion molecule interaction (152). Step 2 is basement membrane break down (31-36 hpf). This process allows the two edges of the CF to fuse together in step 3 (152). At present, there is little knowledge about the initiation or the molecular regulation of this process. Step 3 is tissue fusion of the two edges of the CF (44-52 hpf) (152). This step allows cells to form molecular adhesions, thus creating a fused ventral retina (152). These three steps became vital to this research project, as they offered valuable time frames in which to divide development of the embryos, while knowing specifically what was occurring in the CF at that particular developmental time frame.

Although the eye field may be derived from the anterior neural plate, the eye forms through a series of coordinated and specific interactions between several tissues that are derived from different origins (13,31,153). For this complex coordination to take place, adhesion molecules are vital to hold the two sides of the CF together (152) and regulators such as Rac are needed to promote membrane ruffling to help F-actin spread

during cell-to-cell contact formation (151). Previous work has shown that actin and β-catenin localize at the CF, when the two sides adhere to one another (152). This experiment further indicates that the CF closes in a zipper-like fashion due to its start at the central section or midline then proceeds with the simultaneous outward movement, towards both proximal and distal (152). Prior work demonstrated Rac increases lamellipodial activity increasing the likelihood of E-cadherin engagement (151). If we combine the information from these two studies of actin and β-catenin localization within the eye (152) with observations from cell culture (151), we should observe Rac localization directly proceeding CFC and it would follow along this zipper-like fashion of fusion.

During stage 4, lamination of the seven retinal cell types and RPE, catenin proteins, especially β-catenin, are essential during neurogenesis (154). In a Cre-LoxP system that eliminated or constitutively expressed β-catenin during retinal neurogenesis there were opposing results (154). Elimination of β-catenin presented with lack of differentiation of retinal cell types, likely due to loss of radial arrangements of retinal progenitor cells and abnormal migration of differentiating neurons (154). In these induced mutants, laminar structure and organization was drastically disrupted even though all retinal cell types did form (154). Eliminating β-catenin did not significantly reduce proliferation of RPCs and activating β-catenin did not result in over-proliferation, but a loss of neural retinal identity (154). Ultimately, this study implied that retinal lamination and retinal cell differentiation are genetically separate processes (154).

N-cadherin has also shown to be important for retinal lamination (138). In a *parachute* loss-of-function mutant zebrafish, the retina presents severe lamination defects

and rosette formations, a classic appearance of incorrect and inaccurate adhesion in tissue formation (138). Interestingly, all major cell types appeared to be present and contain a normal number of synapses with typical morphology (138). The lens also develops completely normal, but occasionally, lens epithelia cells become multilayered and take on a rounded shape (138). These results show that cell adhesion, mediated by N-cadherin, is important for retinal lamination and involved in maintaining the lens epithelial sheets (138). While the *parachute* mutant appears to have a coloboma, it has yet to be determined at which stage of CFC there may be defects, if any.

It is apparent from the literature there are a series of proteins and adhesion molecules that are needed to maintain the proper developmental during the 4 stages of vertebrate eye development. Much is needed to determine how the intrinsic regulation of these molecules changes the extrinsic interactions occurring during retinal development.

Summary

Overall, much is known about the developmental stages of the vertebrate eye. How, when, and where many of the structure's originate, what essential pathways are required for proper differentiation, and what molecular integrations are required of cell signaling pathways. Due to early embryonic lethality in many adhesion mutant animal models (139-141), an encompassing knowledge about testing the requirements of these adhesion components in each stage is very difficult, and many questions remain unanswered.

My research is essential, because it provides insight into what cell types and adhesion molecules are vital in preventing eye-related diseases, such as coloboma. I contribute to closing this gap in knowledge by bringing attention to a newly identified

"reaching cell" population present during zebrafish eye development, specifically CFC. This "cell" population could be responsible for adhesion of the two apposed ventral eye tissues that appear at the CFC early stages (1 and 2). Little is known about these stages specifically regarding the role of adhesion molecules and their regulators, such as Rac, during tissue fusion. Based on the genetics of the embryos used during these experiments, this population of "cells" are Rac-dependent while maintaining a retinal derived (*Rx3 positive*) profile. These reaching cells are clearly important, as in their absence coloboma results. While the mechanism and cell type required for basement membrane breakdown is unknown, the reaching cells spatiotemporal presence and dynamics may indicate their potential role in CFC stage 2. Furthermore, the structural interactions and mechanical forces needed for CF fusion process are still open for investigation. These reaching cells provide an exciting possibility for a structural source of a pull force, as well as possible mechanisms for many of the unanswered questions in the field.

CHAPTER II

METHODOLOGY

The purpose of this research is to characterize a group of cells I termed "reaching cells," as I observed them making attachments between multiple tissues. With this research, I had two specific aims with associated questions and hypotheses:

A1 I sought to characterize the appearance and dynamics of reaching cells in a wild-type *Rx3*:GFP zebrafish.

- Q1a) At what developmental time point do the reaching cells first appear during eye development?
- Q1b) What connections do the reaching cells make in the distal section of the eye?
- Q1c) Does this cell population exhibit the same characteristics, such as placement and shape, regardless of developmental time point?

H1 I hypothesized the reaching cells would be present during initiation until completion of CFC, arriving at the eye 24 hours post fertilization (hpf), making the same, if not new connections, to various tissue types in the eye, always displaying the same dynamics regardless of location or developmental time point.

A2 I sought to determine if molecular regulation is required for the spatiotemporal dynamics observed in *Rx3*:GFP reaching cells by utilizing a *hs70l:*Gal4*; UAS:*Rac-DN temporal expression transgenic fish to over-express a dominant negative version of Rac.

H2 I hypothesized that reaching cells would be present during CF closure; however, I predicted that there would be fewer reaching cells within the eye field, in the CF, and the few that are there would not make the same connections as seen in the wild-type (WT).

Fish Husbandry

Fish were maintained according to the ZFIN zebrafish handbook (155-157). In brief, adults were maintained at 28°C on a 14-hour light/10-hour dark cycle. All animals were treated in accordance with established provisions set by the University of Northern Colorado School of Biology Institutional Animal Care and Use Committees (Appendix A).

Only adult fish, 3 months of age or older, were used in breeding. Breeding fish were paired in a divided breeding tank separating males and females. The divider was removed the following morning to ensure the proper observed breed times for desired hours post-fertilization (hpf). A tilting technique was often utilized to encourage close proximity for breeding along with an option of inclined shallow water. The zebrafish (*Danio rerio*) used in this study were of the *Rx3:*GFP strain (unpublished line maintained in A. James lab). These fish were then crossed to a *UAS*:GFP-f2a-Rac^{DN}, or *UAS*:GFP-f2a-Rac^{WT} (158) line, raised to adult hood and then bred to an individual of *Hsp70l:*GAL4^{kca4} transgenic (159,160).

Embryo Collection

Once embryos were collected from a breeding tank, developmental fertilization was verified, and dead and unfertilized eggs disposed. Embryos were separated into petri dishes with a maximum capacity of 50 embryos/dish, provided with fresh fish system water, and placed in an incubator held at 28.5°C in the dark until they reached the appropriate time point for experimentation.

Cryosections

After being euthanized with tricaine at the desired developmental time point, embryos were prepared for cryosectioning (152,160). The frozen block, once taken out of the freezer, was immediately put on ice and carried to the cryostat to prevent thawing. The block was placed immediately into the cryostat and then cut into fourths with a razor blade, using a minimum of one out of four blocks depending on the amount of fish in each block. The frozen block was placed on a cryo-sample holder using Tissue Freezing Media (TFM- VWR, 15148-031), positioned to vertically align with the cryoblade and placed in the cryosection for about 5 minutes while the TFM hardened and turned from clear to white. The sample holder was attached to the chuck, and the chuck's angle adjusted until the angle sliced evenly nasal to temporally. Section thickness was 16-µm.

Immunofluorescence

Cryosections were adhered to positively charged Super Frost slides (VWR, 76204-160) by melting media to slides. Slides were immediately taken to the lab, placed in an immunofluorescent humidity chamber and processed for a modified combination of immunofluorescence protocols followed (152,160). In brief, embryos were placed in block (0.1 % Tx-100; VWR, 97062-208, 1% DMSO, 5% goat serum, VWR, 10152-212). All antibodies and stains were diluted in block. The primary antibody used in this study was mouse anti-Rac (Sigma, R2650), 1:200 dilution. Secondary antibody was goat anti-mouse 488 (Jackson Labs/Sigma, 18772), 1:200. DAPI was applied within the mounting media (Vectashield hard mount w/DAPI; VWR, 101098-044) at the very last step since it also obtained the vectashield as well.

Confocal Imaging-Fixed Imaging

Confocal imaging of fixed cryosections were prepared (152,160). Imaging of cryosections on the confocal were completed as described elsewhere (152). In brief, images were taken on a Zeiss 700 confocal microscope with a 488 laser at a 20X zoom. The entire slide was examined for eye sections that represented each spatial location within the eye (distal, distal central, central, proximal central, proximal). Once located, an optical z-stack was acquired proximal to distal of the full tissue section. Z-stacks ranged from 1-µm to ~ 100-µm thick if and when intact eyes were available. All images were processed identically for brightness and contrast and cropped using Image J software as previously described (152). All images were processed identically within each imaging day (152).

Intensity Measurements

I measured intensity of Rac fluorescence to validate the qualitative observations in Figures 1 and 2. Measurements were taken with a box the size of a single cell (7.179 pixels^2), using Image J. This allowed for collection of a minimum of 5 data points. Five data points were collected since 5 cells is the approximate number of cells comprising the CF. Measurements were taken from the top of the CF to the bottom (ROI3), until at least five data points had been collected at the cellular edge of the CF facing the apposed side.

in vivo imaging studies indicated the CF cells within 5 cell lengths away from the edge (ROI3) are different based on delay of transgenic expression of differentiation markers (161) and nuclear shape differences at the edge versus cells 5+ nuclei away from the CF edge (A. James, unpublished data). Observations that were recorded for ROI2 and ROI4 were at minimum five cells away from the CF seam. Starting from the CF, five

cells were counted in a horizontal direction away from the CF and into the retina. Five data points of background (ROI1) were also collected avoiding collecting any immunofluorescent tissue.

Intensity ratios derived from individual data points were calculated using the mathematical steps below for each individual eye section for each spatiotemporal location.

Step 1: Collected 5 data points from each ROI

Step 2: Averaged 5 background data points for ROI1

$((ROI1_a + ROI1_b + ROI1_c + ROI1_d + ROI1_e)/5$ = averaged background)

Step 3: Subtracted averaged background from each ROI3= adjusted ROI3'

Step 4: Averaged all 5 adjusted ROI3'

$((ROI3'_a + ROI3'_b + ROI3'_c + ROI3'_d + ROI3'_e)/5$ = adjusted averaged ROI3')

Step 5: Steps 1-4 were repeated for ROI2 and ROI4, where ROI1 remained constant throughout each equation as they all were collected from the same image = background adjusted and averaged ROI2' and ROI4'.

Step 6: As minimal difference was observed between ROI2' or ROI4', all individual ROI2' and ROI4' points were averaged to create a full spectrum outside CF measurement (ROI2&4').

Step 7: The average adjusted edge measurement was standardized by the mean of the adjusted measurements on either side of the CF seam = ROI3'/ ROI2&4'

Heat-shock of Embryos for *in vivo* Imaging

Embryos were placed into a PCR tube (6 embryos max per tube approximately 200-µl) using a glass pasteur pipet cut with a diamond cutter. A thermocycler was

utilized to maintain embryos at 28.5°C until the desired experimental heat-shock time (approximately eight hours before desired expression time), then run at 39.5°C for 30 minutes, then returned to 28.5°C until embryos were removed from the PCR tube. Embryos were removed from the PCR tube by squirting fish system water into each one of the PCR tubes and letting the embryos fall into a clean petri dish from the PCR tube.

Embryo Screening

All transgenic embryos were examined under a Leica stereomicroscope using a GFP filter cube for florescence of eyes, heart, and/or body. Embryos that expressed the appropriate fluorescence pattern for each experiment were manually de-chorionated and used for *in vivo* imaging. Florescence in eyes indicates *Rx3*:GFP expression, florescence in heart *hsp70l*;Gal4 presence, and florescence in head/trunk indicates *UAS*:Rac-DN expression. Embryos that were not expressing the appropriate florescence were euthanized immediately after screening.

in vivo Imaging Preparation

Heat-shocked, screened, and appropriate age embryos (times varied for each experiment) were mounted for *in vivo* imaging as previously described (152). In brief, embryos were removed from the petri dish using a wide-mouthed Pasteur glass pipette. Embryos were then placed into the center of a round imaging dish with minimal water and overlaid with an 8:1:1 mixture of fish system water, tricaine (Tricaine- VWR, IC10310680, and low-melt agarose (VWR, 490001-596), respectively. Embryos were then positioned in the agarose using an insect pin to get an appropriate angle on the eye

for confocal imaging. Once the agarose had solidified (about 3-5 minutes) a 1:9 mixture of tricaine and fish system water was applied over the immobilized embryo in the *in vivo* imaging dish.

Confocal Imaging- *in vivo*

Embryos were imaged on the Zeiss 700 confocal microscope using a 40X objective (N.A= 0.8). Images were obtained as an optical z-stack of 1-µm increments encompassing the most outer distal to most inner proximal region of the eye including the forming optic stalk totaling about 100-µm. Optical stacks were then used to separate the eye into fifths, defining the locations (distal, distal central, central, proximal central, proximal). Each stack was used to create a maximum projection to allow for the evaluation of whole cells. In most cases these z-stacks were taken every 15 minutes for four to twelve hours. Individual fish were either imaged during 24-36 hpf or 44-54 hpf.

Post Confocal Imaging – *in vivo*

After imaging was complete, embryos were taken off the scope and transported back to the lab. They were removed from the agar with an insect pin, placed in a petri dish with a wide-mouthed Pasteur glass pipette, and placed in the incubator. Periodically, for a minimum of six-hours, embryos were removed from the incubator and observed under a Leica stereomicroscope for heartbeat, motility, and tap stimulus to ensure vitality was not compromised during the imaging process. Once life had been confirmed, the embryo was placed back in the incubator. Once the minimum six-hour period had ended, the embryo was euthanized, and the video was confirmed to be used in analysis.

Data Analysis of Reaching Cells

All data analyses were performed using Image-J. The *in vivo* imaging (mentioned in section 3.9), were annotated with the draw tool featured in Image-J, so that each reaching cell migration path was traced (*n=3 in vivo* videos). These traced patterns were then overlaid onto a cartoon eye drawing in PowerPoint. A red color was applied to the cartoon drawing to indicate multiple cells had originated from that specific location. If more than one reaching cell had been observed to derive from that area of the eye, but, took a different directional path, an "x" was placed onto the cartoon drawing to depict the starting place of each reaching cell. The developmental hours that the reaching cells were observed were divided into two categories since these time points can be divided into early stages of CFC (24-36 hpf) and late stage CFC (44-54 hpf) (152).

Reaching cell categories were determined by watching *in vivo* videos (total 27-section 3.9) to note distinct cellular shapes and dynamic cellular movements, specifically exhibited by the reaching cell population. I created seven categories, based on the criteria rubric set for each category below. Categories were established when I observed a minimum of three individual cells displaying this phenotype of reaching cell. This could have been three cells within the same video or three cells of the same category within multiple videos. *in vivo* imaging allowed for movies to be taken in frames that were taken at 15 minutes intervals. Videos were also pseudo-colored using image J.

Category 1: short, thin, and wispy, almost appearing like tree branches lacking leaves. The reaching cell is present outside of main retinal tissue for one to three frames, and then retracts. 2-3-μm in length.

Category 2: big and bubbly compared to single cells in retina. Somewhat representative of someone blowing a large bubble of gum. The reaching cell is present outside of main retinal tissue for two to four frames, and then retracts. 2μm in length.

Category 3: long, oblong shape, having an edge with no ripple or bend in the cell membrane. The reaching cell is present outside of main retinal tissue for four frames, and then retracts. 3-5-μm in length.

Category 4: budding yeast-like shape, has a clear bend and or dip in the cell membrane. The reaching cell is present outside of main retinal tissue for two to three frames, and then retracts. 3-5-μm in length.

Category 5: lightning bolt shape. Projects out from the main retinal tissue and then back into the eye field and has a width of at least 2-3-μm. The reaching cell is present outside of main retinal tissue for one frame and then retracts.

Category 6: long wispy cell with a big bubble looking nuclei/cell attached to the very end. Presents similar to neuron phenotype. This cell will travel at least 25-μm. The reaching cell is present outside of main retinal tissue for two or four frames, and then retracts.

Category 7: large, long cell that reaches from one piece of tissue to another. Typically starts small and then grows to a size of about 25-μm wide. The reaching cell is present outside of main retinal tissue for at least five frames, and then retracts. Retina to retina or peripheral edge cells were included in this category.

Rac-GEF Inhibitor

Rac-GEF inhibitor NSC 23766 (Tocris Biosciences; 2161) was used to perform all Rac-GEF inhibitor experiments. All dilutions were made using a serial dilution method. The control had 10 µL of DMSO in 10 mL of fish water. The stock solution was made by 0.05 µg/ml in DMSO. The 538 µg/mL solution had 10 mL of fish water and 10 µL of the stock solution. The 53 µg/mL solution had 1 mL of the 538 µg/mL solution and 9 mL of fish water. The 5.3 µg/mL solution had 1 mL of the 53 µg/mL solution and 4 mL of fish water. After each addition of the inhibitor, the tubes of mixture were vigorously shaken and vortexed in order to mix thoroughly. Embryos of the appropriate developmental period, 40 hpf, were added to the 6-well plate using a glass pasteur pipette. A minimum of six embryos were placed into each well. Embryos were euthanized with tricine at the appropriate developmental time period for observation (52 hpf). Embryos were then fixed as for cryosectioning. Embryos were imaged in a circular *in vivo* imaging dish and positioned in 100% glycerol to acquire the appropriate angle of the eye for imaging. Optical z-stacks were taken similar to *in vivo* imaging with the exception of using time intervals. Once confocal imaging was complete, embryos were imaged on a Lecia stereoscope to measure eye size, body length, and pigmentation.

CHAPTER III

RESULTS

Rac Localizes at Edges of Choroid Fissure Prior to Fusion Markers

Some temporal aspects of CF fusion have been defined in zebrafish. Previous work demonstrated β-catenin and actin colocalize together at the seam of CFC at 47 hpf (152). As development continued at 49 hpf, this strong seam of colocalization progressed outward (distal and proximal sections) in a zipper-like fashion (152). As Rac is required for membrane-ruffling (162) and increases proximity for cadherin proteins to adhere at apposed plasma membranes (151), I sought to determine if Rac localized at leading edges, prior to fusion, as seen in single cell adhesion (151). I hypothesized Rac would have a higher intensity in the proximal central and distal central sections of the eye at 47 hpf proceeding spatiotemporal localization of adhesion markers previously described (152), but within the same spatial directions (outward towards both distal and proximal CF).

WT embryos were cryosectioned at 47 hpf and Rac immunofluorescence was observed for Rac localization through five different sections of the eye, focusing on the CF. Brightfield images were utilized to verify the anatomical location of the five different section of the eye (Figure 1A). A seam of Rac immunofluorescence is present in the proximal central and distal central sections of the eye (Figure 1B).

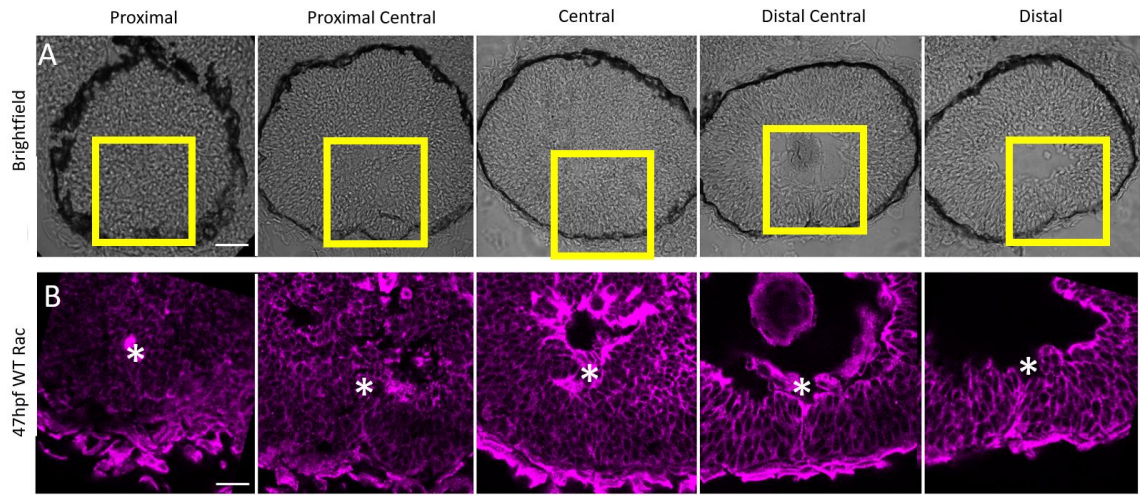

Figure. 1: Heavy Seam of Rac Localization at CF in Proximal Central and Distal Central Sections of the Eye at 47 hpf in Wildtype. Embryos were fixed at 47 hpf and cryosectioned. Confocal images of each sections were observed for Rac localization. Images are representative of A) brightfield anatomical locations of the whole section of the eye, not just the CF. Yellow boxes represent the relative location for B) Rac localization at the CF. Asterisks appear above the CF seam. Images were pseudo-colored purple with image J. Scale bar 25-µm, *n*= minimum of 5 for each section.

Rac is Not Localized with Choroid Fissure During Fusion Events

As Rac is required for the initiation of cell contacts by increasing membrane contacts (151,162) I hypothesized that Rac would dissipate as development progressed into later stages of development, such as 49 hpf, and Rac was no longer utilized in the process of CFC. Rac localization was observed at 49 hpf, when the CF should be fusing within both proximal central and distal central locations (152). WT embryos were cryosectioned at 49 hpf and Rac immunochemistry was used to observe Rac localization through five different sections of the eye, focusing on the CF. Again, brightfield was used

to verify the anatomical location within the eye as a whole (Figure 2A). The Rac seam, previously seen at 47 hpf (Figure 1B), is no longer present at proximal central and distal central sections of the eye (Figure 2B).

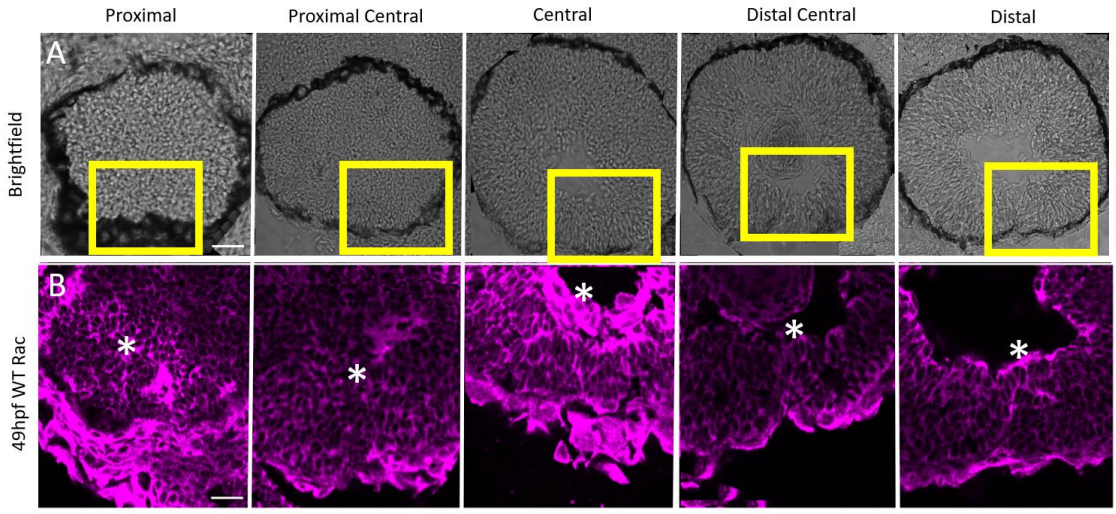

Figure 2: Rac Localization No Longer Present as a Seam in Either Proximal Central or Distal Central Sections of the Eye at 49 hpf in Wildtype. Embryos were fixed at 49 hpf and cryosectioned. Confocal images of each section were observed for Rac localization. Images are representative of A) brightfield anatomical locations of the whole section of the eye. Yellow boxes represent the relative locations of B) Rac localization at the CF. Asterisks indicate the prior location of the seam observed at the 47 hpf. Images were pseudo-colored purple with image J. Scale bar 25-µm. *n*= a minimum of 5 for each section.

Quantification of Rac Fluorescence Intensity at 47/49 hours post-fertilization

Observations from *in vivo* imaging of zebrafish differentiation transgenic marker activation (122) displayed different nuclei orientation of the cells near the CF edge (A. James, unpublished data). I sought to demonstrate the localized differences in Rac localization within and around the CF. To verify the qualitative data, I quantified the intensity of Rac localization at the CF seam as a ratio of mean fluorescence intensity within the CF seam (ROI3', defined as CF edge cells): mean fluorescent intensity

“outside of the CF seam” (ROI2 &4’, defined as cells at minimum 5 nuclei away from the CF edge,). A representation of where image measurements were taken is provided (Figure 3), along with a full description of the ratio calculation (Methods 3.6). Level of mean fluorescence are reduced within the distal central region when comparing measurements at 47 hpf versues 49 hpf (Figure 4). This pattern of reduced Rac florescence over time is most prominent in the proximal central 47 hpf versus 49 hpf indicating Rac intensity dissipates.

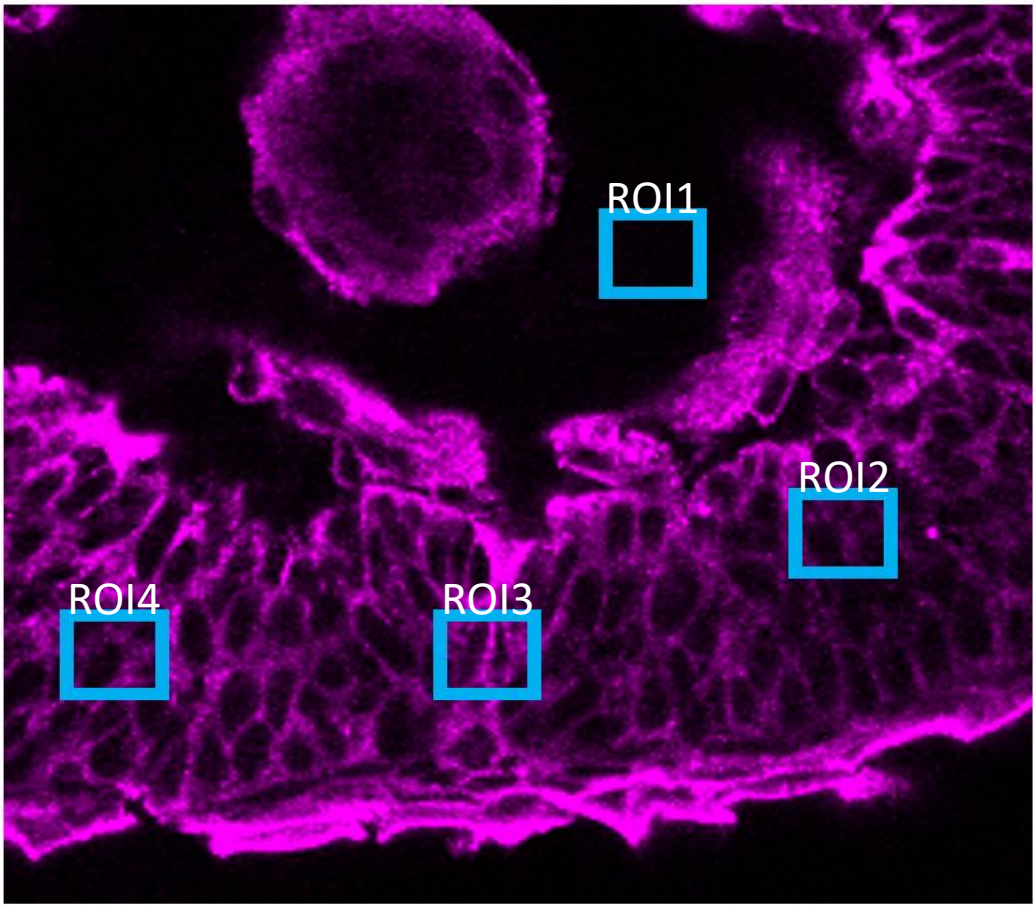

Figure 3: Photographic Illustration of Where Intensity Measurements Were Taken. Boxes depict a relative location where one measurement was taken on one side of the CF seam (ROI4), the opposing side of the seam (ROI2), and in the CF (ROI3). ROI1 represents background. Full description of ratio creation in methods section. Boxes are not to scale, nor represent the exact location where all measurements were taken. Image was pseudo-colored purple with image J.

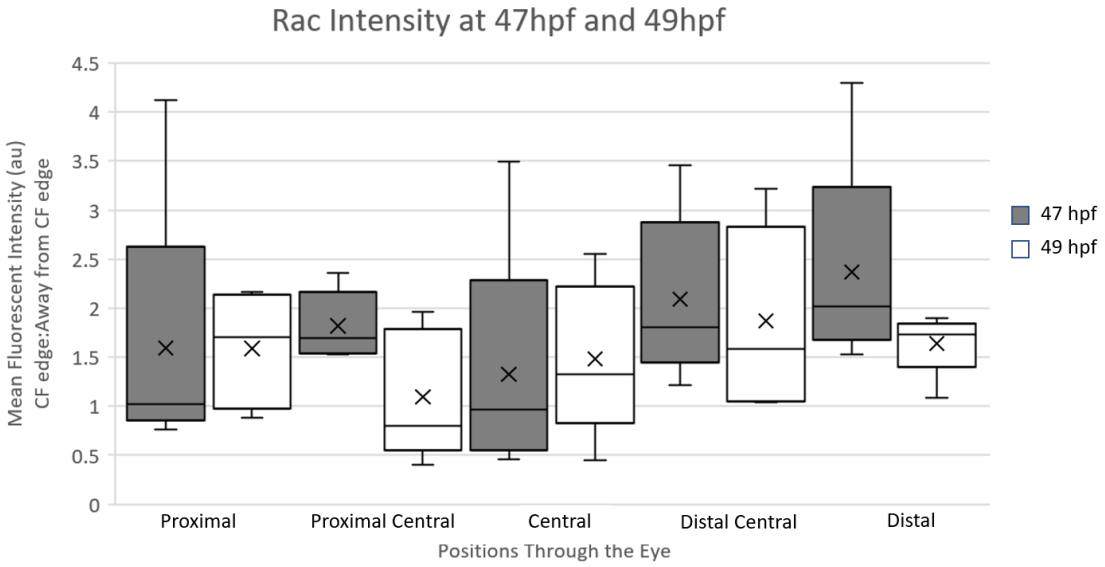

Figure 4: Box Plots of Rac Localization Intensity Ratio at 47 hpf Compared to 49 hpf in 5 Positions of the Eye. Rac intensity immunofluorescence in five replicates are summarized across five locations in the eye. The grey bars represent 47 hpf and the white bars represent 49 hpf. The "X" in each one of the boxes indicates the average of these intensity measurements through each section of the eye at 47 hpf and 49 hpf. Horizontal line in each of the boxes represents the median.

Reaching Cells Are Present in Fixed Tissue at 49 hours post-fertilization

While observing z-stack images of Rac localization, I observed what I have termed a "reaching cell". Observations were made from a 49 hpf embryo that was cryosectiond at 16-µm thick slices, stained for Rac, and imaged using confocal microscopy to take optical 1-µm z-stacks. Reviewing each optical section in progression, I observed a Rac positive connection that stretched from CF side to CF side to lens, touching three distinct locations (asterisks in Figure 5). Although similar cells have been seen in mice models during neural tube closure (163) and in the eye, tethering and pulling the lens into place (85), these are the only documented observations somewhat resembling the cell population I observed (Figure 5). These cells have consistently been

captured *in vivo* via multiple methods of imaging, as well as different individual fish (wildtype, *Rx3*:GFP transgenics, and wildtype membrane-GFP mRNA injected; A. James, unpublished data). Thus, I believe these structures are consistent with development and not an artifact of the stain or an unusual developmental attribute seen in only one embryo.

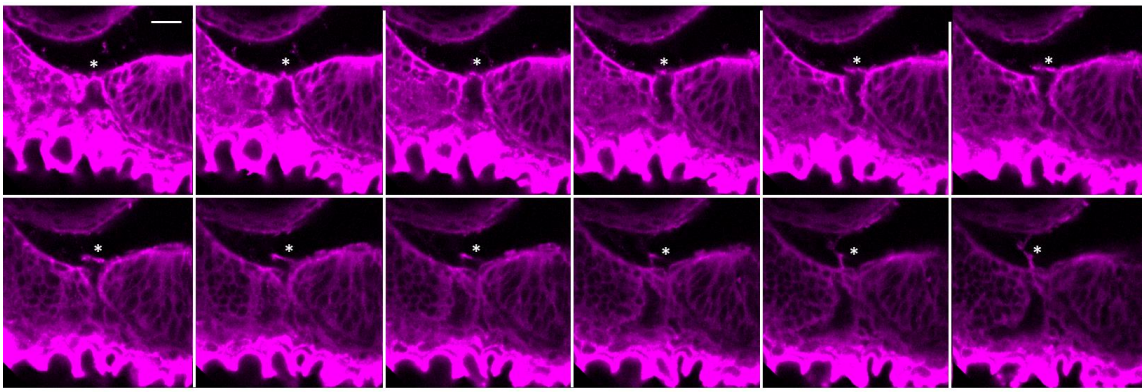

Figure 5: Reaching Cells in Fixed Tissue at 49 hpf Contact Retina to Retina and up to the Lens. Optical z-stack turned into a montage with each image in a serpentine order presenting each 1-μm optical section. Asterisks indicate where the reaching cell is present in the distal central section of the eye of a WT fish at 49 hpf. Images were pseudo-colored purple with image J. Scale bar 25-μm.

Spatiotemporal Appearance of the Reaching Cells in an *Rx3*:GFP Background

In an effort to further understand reaching cells, I sought to identify their location and movements during different developmental windows 24-36 hpf (proliferation and basement membrane breakdown of CFC) and 44-54 hpf (tissue fusion of CFC) that are critical to zebrafish eye development (152). In total, 27 *in vivo* movies were collected of a *Rx3:*GFP background fish line within each time window, representing a minimum of 3 embryos per each full-time window.

When mapping cellular presence and movement dynamics over an eye drawing, I observed an overall shift towards the CF (Figure 6). During the 24-36 hpf reaching cells

were observed to be in the CF, reaching up to the retina, and on the peripheral edges of the eye. As this specific fish line solely labels retina, RPE, and reaching cell population, I do not know the specific presence and location of other specific cell types in the area and therefore cannot rule out that they are in contact with other tissues. As development continued into 44-54 hpf, reaching cells congregate to the CF and away from the peripheral edges as seen in the earlier points. These qualitative data show that earlier in development, the reaching cells span to the outside of the CF and are not isolated to one part of the eye, such as just the CF. These data present a trend within this cell population of earlier hours having a much more dynamic spread of reaching cells over the ventral retina, while later developmental time points seem to have this cell population collecting to and around the CF. These findings encouraged me to observe if the reaching cells present during early time points were exhibiting similar dynamics, such as shape and movement, regardless of location and developmental time point.

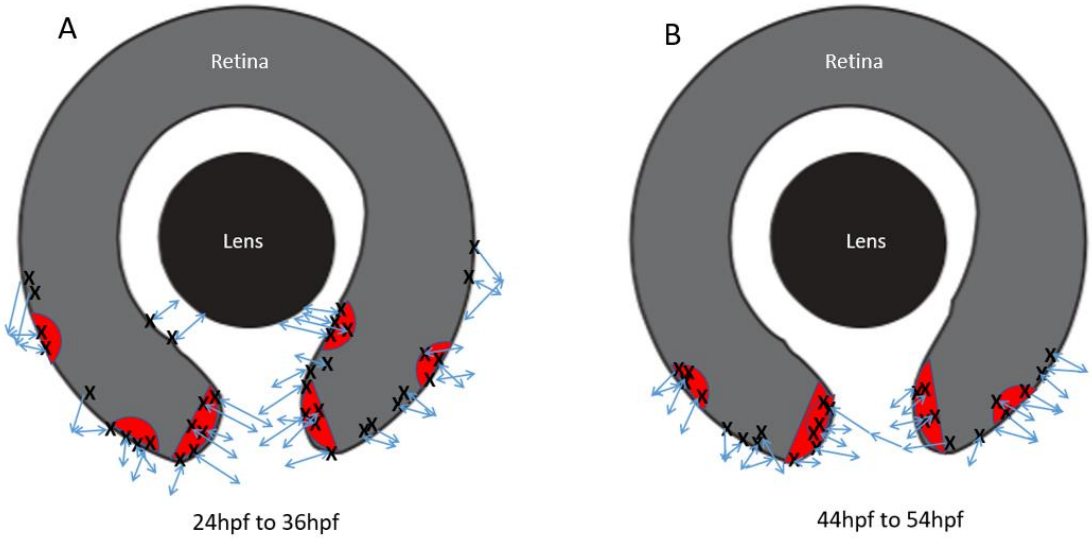

Figure 6: Reaching Cells Progressively Move Towards the CF as Development Proceeds. Cartoon drawing of two eyes at early (A) and late (B) CFC developmental time points. The black circle in each cartoon represents the lens. The grey in each cartoon represents the retina. Reaching cell's path (blue arrows) traced from *in vivo* videos (*n*=3 embryos/time point) and overlaid on the top of the cartoon eye image to denote the paths of the reaching cells. The doubled headed arrows represent the outward and inward motion/path of the reaching cell, however, do not represent a direct measurement of this movement. The single headed arrows represent where the reaching cell originated out of, but did not retract to the same location, however, retracted to a completely different location. The red coloring depicts where more than two reaching cells were seen in the same area. The "x's" denote if more than one reaching cell started in the same area but took a different directional path. Drawing of retina and lens not to scale.

Cellular Dynamics of the Reaching Cells in an *Rx3*:GFP Background

An *Rx3:*GFP background fish line was utilized to image all neural retina derived cells to evaluate the wildtype characteristics of reaching cells. *in vivo* videos were taken and analyzed as described in the methods section (3.7-3.11). Seven categories of reaching cells were identified based on physical shape traits as well as migration dynamics. Categories 1-4 demonstrate obviously different reaching cell shape dynamics from one another, such as wispy branch-like cells (Figure 7- Category 1; *n*=6), bubble-shaped cells (Figure 7- Category 2; *n*=17), an oval-like cell that had a smooth defined cell membrane

(Figure 7- Category 3; *n*=9), and cells that had a budding yeast appearance (Figure 7- Category 4; *n*=12). Categories 1-4 were only observed between the timepoints of 24 hpf-36 hpf (Figure 7; pink square). The most abundant observation was of cells that had the appearance of a lightning bolt (Figure 7- Category 5; *n*=23). Additionally, I observed cells with a long very dynamic, stretchy cell that traveled with a bubble shape attached to the posterior end of the cell (Figure 7- Category 6; *n*=15). Category 7 (Figure 7- Category 7; *n*=6), was only observed in the developmental hours of 44-55 hpf (Figure 7; orange square). This cell category reached from one side of the CF to the other, demonstrating a wide stretching cell, usually located within the CF. Interestingly, categories 5 and 6 were observed in both developmental time points (Figure 7; overlapping squares). While there were similarities seen amongst all 7 categories, these categories were kept separate to show the range of variations observed, as each of these cell categories display a unique difference in behaviors from each other.

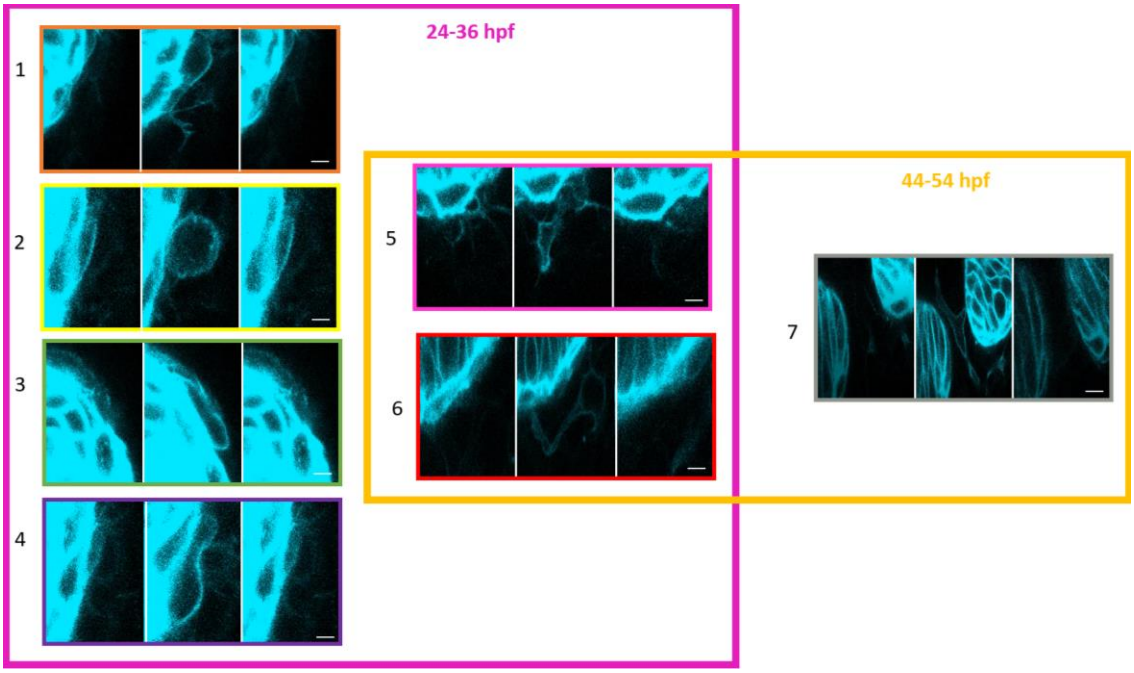

Figure 7: Dynamics of the Reaching Cells Categorizing Based on Cellular Shapes and Dynamics Displayed Along with Timeframes Observed *in vivo*. *Rx3*:GFP embryos were used to perform for all imaging and analysis of cellular dynamic categories. Cells were observed and placed into categories based on behavior and location spatially and temporally. Categories 1-7 represent each of the different categorized cell shapes and behaviors identified. Within each category three images are presented. The left image shows the moment before the reaching cell emerged, the middle picture shows the maximum extension of the reaching cell before it was retracted back to the retina, and the right picture is the moment the reaching cell could no longer be observed. Categories 1-4 were only observed in the 24-36 hpf time frame (pink square). Category 7 was only observed in the 44-54 hpf time frame (orange square). Categories 5 and 6 were observed in both time frames (overlapping squares). Images were pseudo-colored blue with image J. Scale bar 5-µm

Reaching Cells Not Observed in A Dominant Negative Rac Zebrafish

Earlier experiments indicate that WT reaching cells express Rac and therefore may be Rac-dependent (Figure 5). Additionally, prior research showed a possibly similar cell population required for lens placode invagination were still present in a Cre-LoxP inducible Cdc42-knockout (85). To determine if Rac was required for reaching cell dynamics, I utilized a heat shock (HS) inducible Rac dominate-negative, (UAS:GFP-f2a-

RacDN; further referred to as Rac-DN) embryo to reduce overall Rac activity (158). Embryos were HS and screened for Rac-DN expression as described in the methods (3.7-3.10). Initially, Rac-DN expression was induced at 28 hpf to allow reaching cells to arrive at the eye (24 hpf – Figure 6) and observe the requirement of Rac during all stages of CFC beginning at 36 hpf (transition time from basement membrane breakdown to CFC tissue fusion) (152). In three in vivo imaging sessions, no reaching cells were ever observed in the HS induced Rac-DN embryo. I speculate this absence of reaching cells may be due to the timing of HS as cells may have been delayed in their progression inwards towards the CF. I adjusted the HS timepoint at 40 hpf and imaged embryos at 48 hpf in a timeframe where I had regularly observed reaching cells in higher population density. Despite a later Rac-DN HS induction, there were still no reaching cells observed in these videos at later developmental hours (Figure 8B; n= 6 embryo).

In early HS Rac-DN embryos, the OC displayed an unusual boxy-angle, and the cells displayed a cuboidal appearance rather than long and cylindrical, typical of a neuroepithelium structured cell (Figure 8). In late HS embryos, I observed interkinetic nuclear migration that appeared to be stalled (data not shown). I also observed that cells within the RPE divided into the retina, a process that has not been observed in normal eye development as these tissues originate from different tissue origins (fully reviewed in 164). At later HS time points the unusual angle of the OC was resolved along with the unusual cuboidal shape of the cells within the retina (Figure 8B). These embryos also further displayed microphthalmia, shorter overall body length, no yolk separation, and appeared to be developmentally delayed by approximately 8 hours (data not shown).

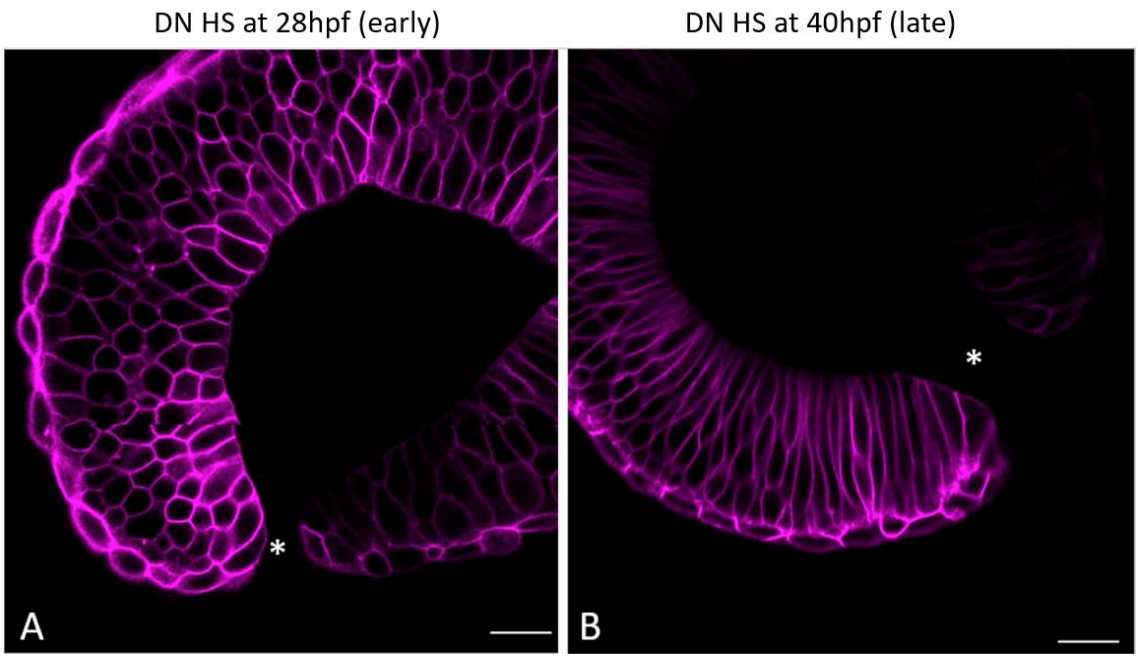

Figure 8: Effects of Early and Late HS Induction of Rac-DN Expression. Embryos were induced to express Rac-DN at either A) early (28 hpf) or B) late (40 hpf) timepoints and imaged under GFP expression 8 hours post HS induction. Reaching cells were never observed in the Rac-DN expressing embryos. Changes in overall cell shape and eye shape were observed only upon early HS induction. There is also an abnormal angle of the OC. Asterisks are to denote where the CF is located. Images were pseudo-colored purple with image J. *n*=7 early, *n*=5 late. Scale bar 25-µm.

Reaching Cells/Rac Activity are Required for Proper CFC

To identify the function of these reaching cells, I utilized a chemical inhibitor of Rac-GEF and observed overall phenotype. Preliminary studies demonstrate when zebrafish embryos are exposed to a Rac-GEF inhibitor (165), they present with a coloboma when the inhibitor was applied at 28 hpf and embryos grown to 55 hpf. In all concentrations tested (530 ug/ml, 53 ug/ml, 5.3 ug/ml), a coloboma was present except in vehicle controls. At lower dilutions (0.5 ug/ml ug/ml) of Rac-GEF inhibitor, colobomas were not as pronounced of a phenotype (open CF) compared to higher dilutions (530.96 ug/ml) of Rac-GEF inhibitor application in which the majority of ventral eye tissue did

not appear present (Figure 9). Additionally, at higher dilutions of Rac-GEF inhibitor the embryo showed microphthalmy, shorter body length, and less pigmentation throughout the body of the embryo (data not shown).

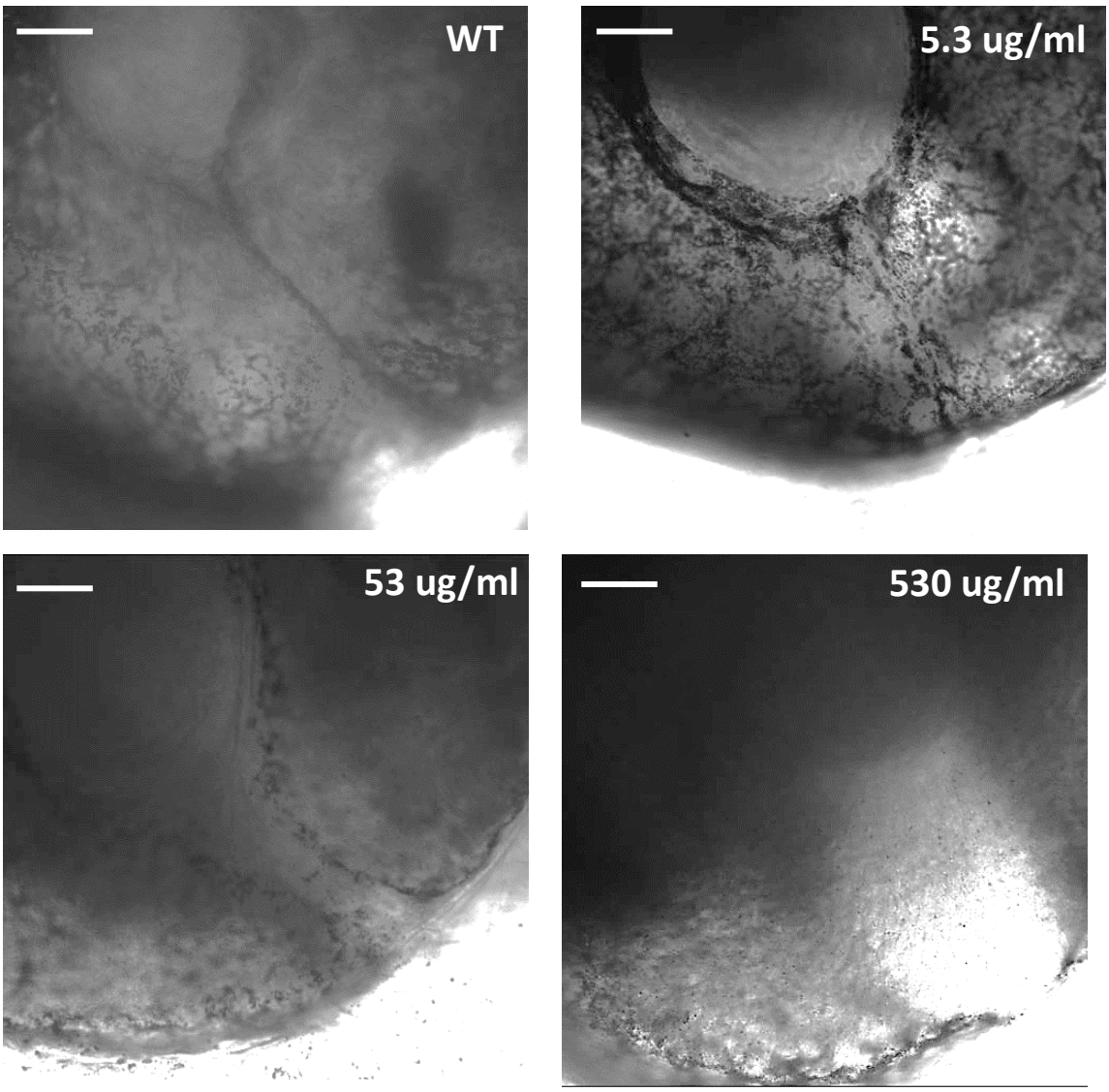

Figure 9: Reaching Cells/Rac Activity are Required for Proper CFC. A serial dilution as performed at different concentrations to reduce Rac activity via a Rac-GEF inhibitor. Higher concentrations show a severe phenotype indicating that Rac/reaching cells are essential for proper CFC. Brightfield is shown in every image. The CF is angled dorsally in the top left corner and ventrally in the bottom left corner in all images. Scale bar 30-µm.

CHAPTER IV

CONCLUSIONS

Rac is a GTPase involved in actin cytoskeleton organization and is critical to polymerization, focal adhesion formation, stress fiber formation, and act to stimulate exchange factors in a variety of signaling pathways (165-167). A previous model proposed Rac localization at the leading edge, which in turn induces lamellipodia activity, thus, increasing cadherin engagement (20,162,168,169). To determine if this model holds true in the tissue level *in vivo,* similar to the single cell level (151), I observed Rac localization during CFC of the zebrafish eye. At 47 hpf, as the two sides of the CF come closer in proximity, there was an abundant seam of Rac present, with high intensity in the Proximal Central section and the Distal Central sections of the eye (Figure 1). As development continues (49 hpf), not but two hours later, the seam that was present at 47 hpf dissipated and Rac mean fluorescent intensity average ratios in these sections had decreased (Figure 1-2 and 4). I believe that is a result of Rac-localization no longer being required to maintain membrane ruffles, in order to bring the two edges of the CF together. It is important to note that in the Proximal and Distal sections, Rac intensity increases at 49 hpf (Figure 4). This data is especially interesting due to the prior work demonstrating the colocalization of actin and β-catenin, components of cellular adhesion, where one section spatially behind Rac (152). This further adds evidence to the proposed model that the CF closes in a zipper-like fashion from the central outwards; both

proximal and distal (152). Collectively these progressive localizations of Rac and subsequent adhesion molecules mimic single cell-to-cell adhesion in a developing tissue.

During analysis, I noted an outlier data point present in each section in both 47 hpf and 49 hpf data sets. As these eye sections were taken from at least 11 different embryos that were set up in different breeds (n=3) and did not come from the same parents or sibling set, it would be inaccurate to say that each section of the eye came from the same embryo. Thus, it is impossible to say that the outlier that is consistent in both data sets is from the same individual, came from the same parents, or came from the same clutch. Regardless, it is clear that there is a trend that as Rac is present at the CF edge preceding tissue fusion spatiotemporal locations and reduces post tissue fusion (proximal central and distal central sections in Figure 1, 2 and 4).

This identification of a reaching cell population is novel to our understanding of the processive nature of CFC. Previously, cellular filapodial extensions were seen in a Cdc42-IRSp53-dependent mouse line (85). I believe this population of mouse lens cells represent a different population from the reaching cells I observed. The mouse lens placode filapodial extensions were observed during lens formation and involved in lens placode tethering (85). The equivalent developmental timeframe for lens placode tethering cell presence is eight hours developmentally prior to when I observed the presence of the reaching cell population around the entire outer ventral retina (Figure 6). Additionally, the mouse lens placode filipodia extensions were only observed to be around the lens, but the reaching cells I observed were not only around the lens, but within the CF connecting the apposed sides of the retina, and along the peripheral edge of the retina. Furthermore, the cell population identified in mice appear to have a reduced

area and appear more string-like in comparison to the reaching cells which appear closer to the size of a complete cell (Figure 7 – Category 2-7). Additionally, cells displaying similar characteristics to the zebrafish reaching cell population have been observed in tissues such as neural tube closure (163) and palate formation (170-177). These cell populations also show different characteristic and behavioral dynamics in the time frame they are present and are not located in the eye. My observation is the first time this cell population has been observed in the zebrafish eye. While it is possible these populations each play a functional role in tissue fusion, I believe zebrafish eye reaching cells are not the same as the cells being observed in other tissues and model organisms.

Zebrafish reaching cells appear to be retinal derived due their *Rx3*:GFP positive labeling with *in vivo* imaging (James and Gross Labs, unpublished data). At this time the reaching cells have not been identified as a specific cell type or the origin of this specific cell type. It is however evident that the reaching cells are Rac dependent as they are not present when Rac activity is reduced (Figure 8). These cells provide an exciting avenue of research in terms of identifying their tissue of origin during development and their functional purpose during CFC as so little is currently known about what cells are involved and/or present during each stage of CFC.

Reaching cells were observed in fixed tissue (Figure 5) and *in vivo* imaging (Figure 7) demonstrating that reaching cells are not an anomaly or specific to one individual embryo or method of observation. These reaching cells were present at the developmental time point of 24 hpf and were continued to be observed until 54 hpf (Figure 6). Reaching cells were predominantly observed in the distal central section of the eye, however, they were seen throughout all five section of the eye. In each of these

sections different events are occurring such as histology, shape changes, and cell patterning (178,179). The discovery of this reaching cell population may indicate the cell type and cellular roles required for proper CFC. The varied categories of reaching cell shapes that I observed (Figure 7) in combination with their alignment to the time frames of proposed steps of zebrafish CFC (152), may indicate shape is related to function.

During stage one (21-31 hpf) tissue proliferations needs to occur to bring the two edges of the CF together (152). During earlier developmental time points (24-36 hpf) as the two edges of the CF are growing closer together (152), reaching cells tended to display a wider range of reaching cells (categories 1-4). The reaching cells are present on the peripheral edges and, reside within the CF. Additionally, reaching cells originate/appear from and retract back into the retina (Figure 6). Categories 1-4 appear to correspond with developmental stages where the two edges of the CF proliferate and come together (152). Categories 1-4 reaching cells are very representative of cells in division and proliferation (Figure 7) (180-183) such as a large bubble shaped cell. It should be noted that both tissue types that marked this cell population are not neural epithelium. However, observation of these cells are displaying signs, such as shape and presumptive origin, that behave like neural epithelium but also cells that are part of the retina.

During stage two (31-36 hpf) the basement membrane is broken down (152), although the mechanism of action is unknown. Interestingly, categories 5 and 6 were present within the time frame when basement membrane breakdown is required (152). Categories 5 and 6 displayed shapes that could be responsible for penetrating/puncturing the basement membrane to allow for breakdown (Figure 7). The shapes observed in

category 5 and 6 are pointy and have a striking motion. It is possible that categories 5 and 6, observed during stage two's time points, are responsible for breaking down the basement membrane. One cellular structure that has a similar role is invadopodia (184), although, these structures have yet to be observed outside of cancer cell lines. In cancer, invadopodia break down the basement membrane, however the endogenous role of invadopodia outside of a tumor is unknown (184-186). It is possible that categories 5 and 6 are invadopodia and are seen for the first time outside of a tumor model, breaking down the basement membrane of the zebrafish eye. Zebrafish eye reaching cell structures appear on a much larger scale than the invadopodia observed in breast cancer cell lines (184).

During stage three (44-52 hpf) tissue fusion of the CF occurs (152). I observed only one reaching cell category present during this time frame (Figure 7 - Category 7). These cells all displayed the same behavior and always met the required guidelines as defined in the rubric (Methods 3.11). Category 7 cell types were only present during the CF tissue fusion (Figure 7) (152) and observed between the two sides of the CF possibly indicative of providing a pull force to both sides of the CF, so fusion may occur. This would be a novel cell type and tension force that has not been previously investigated during CFC.

I have determined Rac is required for the presence and dynamics of reaching cells. When HS induced Rac-DN embryos were observed, no reaching cells were observed at any time point between 22-55 hpf, despite the changes in HS induction timepoints (Figure 8). The shape of the eye, especially the OC, was malformed and had an unusual shape (Figure 8A). Rac-DN embryos furthermore were microphthalmic, had

no yolk separation, were shorter in body length, and appeared developmentally delayed by about eight hours (data not shown). These data indicate Rac may be a key player in the adhesion/migration of the CFC and Rac may play a role in regulating reaching cells.

Preliminary studies utilizing a Rac-GEF inhibitor (187) demonstrated Rac GTPase regulation is required for proper CFC timing. It is possible that this phenotype could be due to delayed development as I noted shorter body length, lacking pigment, and microphthalmic eyes, which are characteristics of 36 hpf (188). In other cytoskeletal regulator mutants, delays were observed in CFC that initiate during basement membrane breakdown although CFC does eventually complete (152). Phenotypes in these mutants were nowhere near as pronounced as though observed in this study (152 versus Figure 9). These data indicate reaching cells and/or Rac activity regulation may be required for proper eye development. Further studies are needed to determine if this was merely a delay or a complete lack of CFC. This datum also supports my hypothesis that tissue fusion utilizes Rac activity similar to single cell adhesion (151).

Collectively the data from this thesis could help identify a mechanism that answers why the CF might fail to close, causing a coloboma. Previous studies highlighted the power of genome editing manipulation to identifying molecular regulators of complex human diseases such as coloboma. Recently, a group sequenced the human genome of patients with coloboma and identified a *mab21L2* mutation, (189). *mab21L2* is thought to be an early downstream effector of Rx3 (189). Upon identification of this gene, TALEN technology was utilized to create specific genetic mutant *C. elegans* and zebrafish embryos that presented with a coloboma (190). These types of studies would be especially useful with a zebrafish model organism since many of the mutants in other

models die at early time points with severe phenotypes (36,43-46). My discovery of these reaching cells could allow for the same opportunity. As the genes and tissues responsible for the reaching cell population are identified, using either human exome sequencing or protein studies could help establish a role of this cell population in eye development, specifically diseases such as coloboma.

While we have made numerous observations regarding this novel reaching cell population during CFC, there are still many new and interesting questions that remain. The identification of this novel population of eye reaching cells has identified a variety of different experiments that are focused on identifying the origin and function of this cell population.

Further experimentation is needed to determine if the reaching cells are in fact cells versus a filapodial/membrane projection. Perhaps my most convincing finding can be seen in category 6, in which you can see GFP expression that appears to be cytoplasmic and surrounding what appears to be a non-fluorescent nucleus (Figure 7). A cleaner experiment would focus on whole mount immunohistochemistry staining actin with phalloidin, nuclei with DAPI, and a Rac antibody. Through such experimentation, one could demonstrate that the reaching "cells" that I observed are cells because each would visibly contain nuclei from a DAPI stain outside of the main retinal tissue. If reaching cells are filapodial extensions (85,191) there would be actin extensions with a phalloidin outline and a complete lack of nuclei inside reaching cells. Distinguishing between these two different possibilities could provide information as to the functional role of this novel cell population present during CFC.

The next step is to determine the tissue source of these cells. Cells appear to be derived from the retina based on their location (Figures 5 and 6) and expression of GFP off of a *Rx3* promoter (56,58,), however, I did not observe the cell populations specific tissue origination.

Unfortunately, simply observing *Rx3*:GFP expression does not identify the specific tissue from which the reaching cells were derived as *Rx3* is responsible for labeling the neural tissue, retinal tissue, and RPE in early development (56,58). This method would also lack in the ability to identify where exactly the insertion was made into the genome when the transgenic was made, so it is possible a genetic enhancer is causing off-target effects for expression which means it might not be any of the tissue types listed above (192). Fate mapping studies using HS-induced Kaede fish (193) in an *Rx3*:GFP background line would allow me to view neural retina morphogenesis and backtrack exactly where and when the cells originate and their path of migration, if any. Identification of the origin of location could then be utilized to isolate these cells via Fluorescent Activated Cell Sorting, which could then be utilized for RNA-sequencing to define these cells transcriptionally (194). This protocol however requires that the embryo be dissociated to create single cells to sort, thus losing the location information. These cells could further be vital to our understanding of wound healing, especially if they are actively involved in pulling two tissues edges together.

While we were able to determine Rac activity is required for both reaching cell presence (Figure 8), dynamics (Figure 7), and proper CFC (Figure 8), further studies are needed to specifically identify the requirement for each category type of reaching cell (Figure 7). This could be accomplished using localized and/or single-cell HS induction

(195) of Rac-DN embryos to further determine phenotypes due to lack of specific reaching cell(s) versus complete reduction of Rac throughout the entire embryo (Figure 8).

While I was unable to work with the HS induced Constitutively Active version of Rac (Rac-CA; (158)), these embryos could be utilized to determine if more reaching cells are created due to the overexpression of Rac activity. Previous work in chicken embryonic fibroblast cell cultures demonstrated that when Rac was overexpressed there was a link between Rac protein distribution and the unique effect Rac has on the actin cytoskeleton organization (196). It is possible HS-induced Rac-CA expression in zebrafish reaching cell population could lead to increased protrusive activity. If the function of these reaching cells is to initiate CFC, whether they are responsible for breakdown of the basement membrane or actively being involved in pulling the two sides of the CF together, I expect CFC may occur at a faster rate than observed in the WT. It is also possible increased Rac activity (Rac-CA) could have the reverse effect and slow down development as competition for binding sites or decreased time for cadherin engagement would reduce tissue fusion, possibly creating a coloboma.

REFERENCES

1. Chia EM, Mitchell P, Ojaimi E, Rochtchina E, Wang JJ. Assessment of vision-related quality of life in an older population subsample: The Blue Mountains Eye Study. *Ophthalmic Epidemiol*. 2006;13(6):371–377.

2. Langelaan M, de Boer MR, van Nispen RM, Wouters B, Moll AC, van Rens GH. Impact of visual impairment on quality of life: a comparison with quality of life in the general population and with other chronic conditions. *Ophthalmic Epidemiol*. 2007;14(3):119–126.

3. Author Anonymous. 2010. The Lighthouse International Homepage. The International Agency for the Prevention of Blindness. <https://www.iapb.org/member/lighthouse-international/>. Accessed 25 July 2018.

4. Author Anonymous. 2008. Autism and Blindness Homepage. Nebraska Center for the Education of Children who are blind or visually Impaired. <https://web.archive.org/web/20080808120836/http:/www.ncecbvi.org/autism.htm>. Accessed 27 May 2018.

5. Author Anonymous. 2008. Circadian Rhythm Sleep Disorder Homepage. American Academy of Sleep Medicine. <https://web.archive.org/web/20100826121447/http:/www.aasmnet.org/Resources/FactSheets/CRSD.pdf>. Accessed 26 June 2018.

6. Sack RL, Lewy AJ, Blood ML, Keith LD, Nakagawa H. Circadian rhythm abnormalities in totally blind people: incidence and clinical significance. *J Clin Endocrinol Metab*. 1992;75(1):127–134.

7. Lamoureux E, Pesudovs K. Vision-specific quality-of-life research: a need to improve the quality. *Am J Ophthalmol*. 2011;151(2):195–7.e2.

8. Breland F. and Midgley K. 2010. Promoting Healthy Vision Development: The American Optometric Association's InfantSee Program Homepage. The Urban Child Institute. < http://www.urbanchildinstitute.org/sites/all/files/2010-06-Infant_Vision_Brief.pdf>. Accessed 1 May 2018.

9. Bermejo E, Martínez-Frías ML. Congenital eye malformations: clinical-epidemiological analysis of 1,124,654 consecutive births in Spain. *Am J Med Genet*. 1998;75(5):497–504.

10. Stoll C, Alembik Y, Dott B, Roth MP. Congenital eye malformations in 212,479 consecutive births. *Ann Genet*. 1997;40(2):122–128.

11. Huynh TP, Mann SN, Mandal NA. Botanical compounds: effects on major eye diseases. *Evid Based Complement Alternat Med*. 2013;2013:549174.

12. Chang L, Blain D, Bertuzzi S, Brooks BP. Uveal coloboma: clinical and basic science update. *Curr Opin Ophthalmol*. 2006;17(5):447–470.

13. Gestri G, Bazin-Lopez N, Scholes C, Wilson SW. Cell Behaviors during Closure of the Choroid Fissure in the Developing Eye. *Front Cell Neurosci*. 2018;12:42.

14. Onwochei BC, Simon JW, Bateman JB, Couture KC, Mir E. Ocular colobomata. *Surv Ophthalmol*. 2000;45(3):175–194.

15. Sanyanusin P, Schimmenti LA, McNoe LA, et al. Mutation of the PAX2 gene in a family with optic nerve colobomas, renal anomalies and vesicoureteral reflux [published correction appears in Nat Genet. 1996 May;13(1):129]. *Nat Genet*. 1995;9(4):358–364.

16. Favor, J., Gloeckner, C. J., Neuhäuser-Klaus, A., Pretsch, W., Sandulache, R., Saule, S., & Zaus, I. Relationship of Pax6 activity levels to the extent of eye development in the mouse, Mus musculus. *Genetics*. 2008;179(3):1345–1355.

17. Hallonet M, Hollemann T, Pieler T, Gruss P. Vax1, a novel homeobox-containing gene, directs development of the basal forebrain and visual system. *Genes Dev*. 1999;13(23):3106–3114.

18. Lee J, Gross JM. Laminin beta1 and gamma1 containing laminins are essential for basement membrane integrity in the zebrafish eye. *Invest Ophthalmol Vis Sci*. 2007;48(6):2483–2490.

19. Bryan CD, Chien CB, Kwan KM. Loss of laminin alpha 1 results in multiple structural defects and divergent effects on adhesion during vertebrate optic cup morphogenesis. *Dev Biol*. 2016;416(2):324–337.

20. Nüsslein-Volhard C. The zebrafish issue of Development. *Development*. 2012;139(22):4099–4103.

21. Bibliowicz, J., Tittle, R. K., & Gross, J. M. Toward a better understanding of human eye disease insights from the zebrafish, Danio rerio. *Progress in molecular biology and translational science*. 2011:100:87–330.

22. Dooley K. and Lenard Z. 2000. Current Opinion in genetics and development. Science Direct Elsevier volume:10, issue 3, pg. 252-256.

23. Zagozewski JL, Zhang Q, Eisenstat DD. Genetic regulation of vertebrate eye development. *Clin Genet*. 2014;86(5):453–460.

24. Lekven AC, Thorpe CJ, Waxman JS, Moon RT. Zebrafish wnt8 encodes two wnt8 proteins on a bicistronic transcript and is required for mesoderm and neurectoderm patterning. *Dev Cell*. 2001;1(1):103–114.

25. Erter CE, Wilm TP, Basler N, Wright CV, Solnica-Krezel L. Wnt8 is required in lateral mesendodermal precursors for neural posteriorization in vivo. *Development*. 2001;128(18):3571–3583

26. Kiecker C, Niehrs C. A morphogen gradient of Wnt/beta-catenin signalling regulates anteroposterior neural patterning in Xenopus. *Development*. 2001;128(21):4189–4201

27. Heisenberg, C. P., Houart, C., Take-Uchi, M., Rauch, G. J., Young, N., Coutinho, P., Masai, I., Caneparo, L., Concha, M. L., Geisler, R., Dale, T. C., Wilson, S. W., & Stemple, D. L. (2001). A mutation in the Gsk3-binding domain of zebrafish Masterblind/Axin1 leads to a fate transformation of telencephalon and eyes to diencephalon. *Genes & development*, *15*(11), 1427–1434.

28. Martinez G, Wijesinghe M, Turner K, et al. Conditional mutations of beta-catenin and APC reveal roles for canonical Wnt signaling in lens differentiation. *Invest Ophthalmol Vis Sci*. 2009;50(10):4794–4806.

29. Smith AN, Miller LA, Song N, Taketo MM, Lang RA. The duality of beta-catenin function: a requirement in lens morphogenesis and signaling suppression of lens fate in periocular ectoderm. *Dev Biol*. 2005;285(2):477–489.

30. Zuber ME, Gestri G, Viczian AS, Barsacchi G, Harris WA. Specification of the vertebrate eye by a network of eye field transcription factors. *Development*. 2003;130(21):5155–5167.

31. Zuber ME, Perron M, Philpott A, Bang A, Harris WA. Giant eyes in Xenopus laevis by overexpression of XOptx2. *Cell*. 1999;98(3):341–352.

32. Mathers PH, Grinberg A, Mahon KA, Jamrich M. The Rx homeobox gene is essential for vertebrate eye development. *Nature*. 1997 Jun 5; 387(6633):603-7.

33. Chow RL, Altmann CR, Lang RA, Hemmati-Brivanlou A. Pax6 induces ectopic eyes in a vertebrate. *Development*. 1999;126(19):4213–4222

34. Lavado A, Lagutin OV, Oliver G. Six3 inactivation causes progressive caudalization and aberrant patterning of the mammalian diencephalon. *Development*. 2008;135(3):441–450.

35. Carl M, Loosli F, Wittbrodt J. Six3 inactivation reveals its essential role for the formation and patterning of the vertebrate eye. *Development*. 2002;129(17):4057–4063.

36. Porter FD, Drago J, Xu Y, Cheema SS, Wassif C, Huang SP, Lee E, Grinberg A, Massalas JS, Bodine D, Alt F, Westphal H. Lhx2, a LIM homeobox gene, is required for eye, forebrain, and definitive erythrocyte development. *Development*. 1997 Aug; 124(15):2935-44.

37. Loosli, F., Winkler, S., & Wittbrodt, J. (1999). Six3 overexpression initiates the formation of ectopic retina. *Genes & development*, *13*(6), 649–654.

38. Stigloher C, Ninkovic J, Laplante M, Geling A, Tannhäuser B, Topp S, Kikuta H, Becker TS, Houart C, Bally-Cuif L. Segregation of telencephalic and eye-field identities inside the zebrafish forebrain territory is controlled by Rx3. *Development*. 2006 Aug; 133(15):2925-35.

39. Maurus D, Héligon C, Bürger-Schwärzler A, Brändli AW, Kühl M. Noncanonical Wnt-4 signaling and EAF2 are required for eye development in Xenopus laevis. *EMBO J*. 2005;24(6):1181–1191.

40. Martinez-Morales JR, Wittbrodt J. Shaping the vertebrate eye. *Curr Opin Genet Dev*. 2009 Oct; 19(5):511-7.

41. Rembold M, Loosli F, Adams RJ, Wittbrodt J. Individual cell migration serves as the driving force for optic vesicle evagination. *Science*. 2006;313(5790):1130–1134.

42. Loosli F, Köster RW, Carl M, Krone A, Wittbrodt J. Six3, a medaka homologue of the Drosophila homeobox gene sine oculis is expressed in the anterior embryonic shield and the developing eye. *Mech Dev*. 1998;74(1-2):159–164.

43. Chiang C, Litingtung Y, Lee E, et al. Cyclopia and defective axial patterning in mice lacking Sonic hedgehog gene function. *Nature*. 1996;383(6599):407–413.

44. Chou SJ, Tole S. Lhx2, an evolutionarily conserved, multifunctional regulator of forebrain development. *Brain Res*. 2019;1705:1–14.

45. Geng X, Speirs C, Lagutin O, et al. Haploinsufficiency of Six3 fails to activate Sonic hedgehog expression in the ventral forebrain and causes holoprosencephaly. *Dev Cell*. 2008;15(2):236–247.

46. Wallis DE, Roessler E, Hehr U, et al. Mutations in the homeodomain of the human SIX3 gene cause holoprosencephaly. *Nat Genet*. 1999;22(2):196–198.

47. Gal, J. S., Morozov, Y. M., Ayoub, A. E., Chatterjee, M., Rakic, P., & Haydar, T. F. Molecular and morphological heterogeneity of neural precursors in the mouse neocortical proliferative zones. *The Journal of neuroscience.* 2006;26(3), 1045–1056.

48. Wang, W. L., Li, Q., Xu, J., & Cvekl, A. Lens fiber cell differentiation and denucleation are disrupted through expression of the N-terminal nuclear receptor box of NCOA6 and result in p53-dependent and p53-independent apoptosis. *Molecular biology of the cell*. 2010;21(14), 2453–2468.

49. Cavodeassi, F., Creuzet, S., & Etchevers, H. C. The hedgehog pathway and ocular developmental anomalies. *Human genetics*. 2019;138(8-9), 917–936.

50. Morcillo J, Martínez-Morales JR, Trousse F, Fermin Y, Sowden JC, Bovolenta P. Proper patterning of the optic fissure requires the sequential activity of BMP7 and SHH. *Development.* 2006;133(16):3179-90.

51. Gongal PA, French CR, Waskiewicz AJ. Aberrant forebrain signaling during early development underlies the generation of holoprosencephaly and coloboma. *Biochim Biophys Acta*. 2011;1812(3):390-401.

52. Barishak YR. Embryology of the eye and its adnexae. *Dev Ophthalmol.* 1992; 24:1-142.

53. Martí E, Bovolenta P. Sonic hedgehog in CNS development: one signal, multiple outputs. *Trends Neurosci.* 2002; 25(2): 89–96

54. Gallardo V, Bovolenta P. Positive and negative regulation of Shh signaling in vertebrate retinal development. *Faculty* Rev. 2018;7:F1000 -1934.

55. Svoboda KK, O'Shea KS. An analysis of cell shape and the neuroepithelial basal lamina during optic vesicle formation in the mouse embryo. *Development*. 1987;100(2):185-200.

56. Kennedy BN, Stearns GW, Smyth VA, et al. Zebrafish rx3 and mab21l2 are required during eye morphogenesis. *Dev Biol*. 2004;270(2):336–349.

57. Andreazzoli M, Gestri G, Angeloni D, Menna E, Barsacchi G. Role of Xrx1 in Xenopus eye and anterior brain development. *Development*. 1999;126(11):2451–2460.

58. Loosli F, Staub W, Finger-Baier KC, et al. Loss of eyes in zebrafish caused by mutation of chokh/rx3. *EMBO Rep*. 2003;4(9):894–899.

59. Furukawa T, Morrow EM, Cepko CL. Crx, a novel otx-like homeobox gene, shows photoreceptor-specific expression and regulates photoreceptor differentiation. *Cell*. 1997;91(4):531–541.

60. Stigloher C, Ninkovic J, Laplante M, Geling A, Tannhäuser B, Topp S, Kikuta H, Becker TS, Houart C, Bally-Cuif L. Segregation of telencephalic and eye-field identities inside the zebrafish forebrain territory is controlled by Rx3. *Development*. 2006;133(15):2925-35.

61. Winkler S, Loosli F, Henrich T, Wakamatsu Y, Wittbrodt J. The conditional medaka mutation eyeless uncouples patterning and morphogenesis of the eye. *Development.* 2000;127(9):1911-9.

62. Medina-Martinez O, Amaya-Manzanares F, Liu C, Mendoza M, Shah R, Zhang L, Behringer RR, Mahon KA, Jamrich M . Cell-autonomous requirement for rx function in the mammalian retina and posterior pituitary. *PLoS One*. 2009;4(2):e4513

63. Brown KE, Keller PJ, Ramialison M, Rembold M, Stelzer EH, Loosli F, Wittbrodt J. Nlcam modulates midline convergence during anterior neural plate morphogenesis. *Dev Biol.* 2010;339(1):14-25.

64. Sjodal M, Edlund T, Gunhaga L. Time of exposure to BMP signals plays a key role in the specification of the olfactory and lens placodes ex vivo. *Dev Cell.* 2007;13:141–149

65. Chapman SC, Schubert FR, Schoenwolf GC, Lumsden A. Analysis of spatial and temporal gene expression patterns in blastula and gastrula stage chick embryos. *Dev Biol*. 2002; 245(1):187-99.

66. Bailey AP, Bhattacharyya S, Bronner-Fraser M, Streit A. Lens specification is the ground state of all sensory placodes, from which FGF promotes olfactory identity. *Dev Cell*. 2006;11(4):505-17.

67. Dudley AT, Robertson EJ. Overlapping expression domains of bone morphogenetic protein family members potentially account for limited tissue defects in BMP7 deficient embryos. *Dev Dyn.* 1997;208(3):349-62.

68. Furuta Y, Hogan BL. BMP4 is essential for lens induction in the mouse embryo. *Genes Dev.* 1998;12(23):3764-75.

69. Wawersik S, Purcell P, Rauchman M, Dudley AT, Robertson EJ, Maas R. BMP7 acts in murine lens placode development. *Dev Biol.* 1999;207(1):176-88.

70. Huang J, Liu Y, Filas B, Gunhaga L, Beebe DC. Negative and positive auto-regulation of BMP expression in early eye development. *Dev Biol*. 2015;407(2):256–264.

71. Fuhrmann S. Eye morphogenesis and patterning of the optic vesicle. *Curr Top Dev Biol*. 2010;93:61–84.

72. Graw J. Eye development. *Curr Top Dev Biol*. 2010;90:343–386.

73. Satoru Sasagawa, Takashi Takabatake, Yuka Takabatake, Tatsuo Muramatsu, Kazuhito Takeshima. Axes establishment during eye morphogenesis in Xenopus by coordinate and antagonistic actions of BMP4, Shh, and RA. *Genesis the Journal of Genetics and Development.* 2002;2(3):86-96.

74. Cepko, C. L., Austin, C. P., Yang, X., Alexiades, M. and Ezzeddine, D. Cell fate determination in the vertebrate retina. *Proc. Natl. Acad. Sci. USA.* 1996;93,589-595.

75. Golub R, Adelman Z, Clementi J, Weiss R, Bonasera J, Servetnick M. Evolutionarily conserved and divergent expression of members of the FGF receptor family among vertebrate embryos, as revealed by FGFR expression patterns in Xenopus. *Dev Genes Evol*. 2000;210(7):345–357.

76. Lea R, Papalopulu N, Amaya E, Dorey K. Temporal and spatial expression of FGF ligands and receptors during Xenopus development. *Dev Dyn*. 2009;238(6):1467–1479.

77. Pope AP, Liu C, Sater AK, Serventnick M.FGFR3 expression in Xenopus laevis. *Gene Expression Patterns*. 2009;10:87-92

78. Ornitz, D. M., & Itoh, N. The Fibroblast Growth Factor signaling pathway. *Wiley interdisciplinary reviews. Developmental biology*. 2015;*4*(3), 215–266.

79. Yamanaka Y, Lanner F, Rossant J.Development. FGF signal-dependent segregation of primitive endoderm and epiblast in the mouse blastocyst. *2010;137(5):715-24.*

80. Trokovic R, Jukkola T, Saarimäki J, Peltopuro P, Naserke T, Weisenhorn DM, Trokovic N, Wurst W, Partanen J. Fgfr1-dependent boundary cells between developing mid- and hindbrain. *Dev Biol. 2005; 278(2):428-39.*

81. Blak AA, Naserke T, Saarimäki-Vire J, Peltopuro P, Giraldo-Velasquez M, Vogt Weisenhorn DM, Prakash N, Sendtner M, Partanen J, Wurst W. Fgfr2 and Fgfr3 are not required for patterning and maintenance of the midbrain and anterior hindbrain. *Dev Biol.* 2007; 303(1):231-43.

82. A. Picker, F. Cavodeassi, A. Machate, S. Bernauer, S. Hans, G. Abe, K. Kawakami, S.W. Wilson, M. Brand Dynamic coupling of pattern formation and morphogenesis in the developing vertebrate retina. *PLoS Biol*. 2009;p. e1000214
83. Hartsock, A., Lee, C., Arnold, V., and J. Gross. Hyaloid vasculature formation in zebrafish does not require the lens for recruitment of vascular precursor cells. *Developmental Biology.* 2014;394 (2), 327-39.

84. Brady RC, Hilfer SR. Optic cup formation: a calcium-regulated process. *Proc Natl Acad Sci USA.* 1982;79(18):5587-91.

85. Chauhan BK, Disanza A, Choi SY, Faber SC, Lou M, Beggs HE, Scita G, Zheng Y, Lang RA. Cdc42- and IRSp53-dependent contractile filopodia tether presumptive lens and retina to coordinate epithelial invagination. *Development.* 2009;136(21):3657-67.

86. Mertes F, Martinez-Morales JR, Nolden T, Spörle R, Wittbrodt J, Lehrach H, Himmelbauer H. Cloning of mouse ojoplano, a reticular cytoplasmic protein expressed during embryonic development. *Gene Expr Patterns*. 2009*;9(8):562-7.*

87. Hyer J, Kuhlman J, Afif E, Mikawa T. Optic cup morphogenesis requires pre-lens ectoderm but not lens differentiation. *Dev Biol.* 2003;259(2):351-63.

88. Smith AN, Miller LA, Radice G, Ashery-Padan R, Lang RA. Stage-dependent modes of Pax6-Sox2 epistasis regulate lens development and eye morphogenesis. *Development.* 2009;136(17):2977-85.

89. Nishihara, D., Yajima, I., Tabata, H., Nakai, M., Tsukiji, N., Katahira, T., Yamamoto, H. Otx2 is involved in the regional specification of the developing retinal pigment epithelium by preventing the expression of sox2 and fgf8, factors that induce neural retina differentiation. *PloS one*. 2012;7(11), e48879.

90. Hirashima M, Kobayashi T, Uchikawa M, Kondoh H, Araki M. Anteroventrally localized activity in the optic vesicle plays a crucial role in the optic development. *Dev Biol.* 2008;317(2):620-31.

91. Kagiyama Y, Gotouda N, Sakagami K, Yasuda K, Mochii M, Araki M. Extraocular dorsal signal affects the developmental fate of the optic vesicle and patterns the optic neuroepithelium. *Dev Growth Differ.* 2005;47(8):523-36.

92. Differentiation of lens and pigment cells in cultures of neural retinal cells of early chick embryos. *Araki M, Okada TS. Dev Biol. 1977 Oct 1; 60(1):278-86.*

93. Clayton R, et al. Experimental manipulation of alternative pathways of differentiation in cultures of embryonic chick neural retina. Development Growth & Differentiation. 1977;19:319–328.
94. Horsford DJ, Nguyen MT, Sellar GC, Kothary R, Arnheiter H, McInnes RR. Chx10 repression of Mitf is required for the maintenance of mammalian neuroretinal identity. *Development.* 2005;132(1):177-87.

95. Itoh Y, et al. The differentiation of pigment cells in cultures of chick embryonic neural retinae. Development Growth & Differentiation. 1975;17:39–50.

96. Opas M, Davies JR, Zhou Y, Dziak E. Formation of retinal pigment epithelium in vitro by transdifferentiation of neural retina cells. *Int J Dev Biol.* 2001;45(4):633-42.

97. Rowan S, Chen CM, Young TL, Fisher DE, Cepko CL. Transdifferentiation of the retina into pigmented cells in ocular retardation mice defines a new function of the homeodomain gene Chx10. *Development.* 2004;131(20):5139-52.

98. Westenskow PD, McKean JB, Kubo F, Nakagawa S, Fuhrmann S. Ectopic Mitf in the embryonic chick retina by co-transfection of β-catenin and Otx2. *Invest Ophthalmol Vis Sci.* 2010;51(10):5328-35.

99. Coulombre JL, Coulombre AJ. Regeneration of neural retina from the pigmented epithelium in the chick embryo. *Dev Biol.* 1965;12(1):79-92.

100. Reh TA, Pittack C. Semin. Transdifferentiation and retinal regeneration. *Cell Biol.* 1995;6(3):137-42.

101. Stroeva OG, Mitashov VI. Retinal pigment epithelium: proliferation and differentiation during development and regeneration. *Int Rev Cytol*. 1983;83:221–293.

102. Hirashima M, Kobayashi T, Uchikawa M, Kondoh H, Araki M. Anteroventrally localized activity in the optic vesicle plays a crucial role in the optic development. *Dev Biol.* 2008;317(2):620-31.

103. Yun S, Saijoh Y, Hirokawa KE, Kopinke D, Murtaugh LC, Monuki ES, Levine EM. Lhx2 links the intrinsic and extrinsic factors that control optic cup formation. *Development.* 2009;136(23):3895-906.

104. Strauss O. The retinal pigment epithelium in visual function. *Physiol Rev.* 2005;85(3):845-81

105. Bharti K, Nguyen MT, Skuntz S, Bertuzzi S, Arnheiter H. The other pigment cell: specification and development of the pigmented epithelium of the vertebrate eye. *Pigment Cell Res.* 2006;19(5):380-94.

106. Bumsted KM, Barnstable CJ. Dorsal retinal pigment epithelium differentiates as neural retina in the microphthalmia (mi/mi) mouse. *Invest Ophthalmol Vis Sci.* 2000;41(3):903-8

107. Martinez-Morales JR, Signore M, Acampora D, Simeone A, Bovolenta P. Otx genes are required for tissue specification in the developing eye. *Development.* 2001;128(11):2019-30.

108. Nguyen M, Arnheiter H. Signaling and transcriptional regulation in early mammalian eye development: a link between FGF and MITF. *Development.* 2000;127(16):3581-91.

109. Raymond SM, Jackson IJ. The retinal pigmented epithelium is required for development and maintenance of the mouse neural retina. *Curr Biol.* 1995;5(11):1286-95.

110. Scholtz CL, Chan KK. Complicated colobomatous microphthalmia in the microphthalmic (mi/mi) mouse. *Development.* 1987;99(4):501-8.

111. Hero, I. Optic fissure closure in the normal cinnamon mouse. An ultrastructural study. *Invest Ophthalmol Vis Sci.* 1990;31,197–216.

112. García-Llorca, A., Aspelund, S. G., Ogmundsdottir, M. H., Steingrimsson, E., & Eysteinsson, T. The microphthalmia-associated transcription factor (Mitf) gene and its role in regulating eye function. *Scientific reports*. 2019;*9*(1), 15386.

113. Rojas-Muñoz A, Dahm R, Nüsslein-Volhard C. chokh/rx3 specifies the retinal pigment epithelium fate independently of eye morphogenesis. *Dev Biol*. 2005;288(2):348–362.

114. Dowling J. E. 1987. The Retina: An Approachable Part of the Brain? Cambridge: Harvard University Press.

115. Hammer M, Roggan A, Schweitzer D, Müller G. Optical properties of ocular fundus tissues--an in vitro study using the double-integrating-sphere technique and inverse Monte Carlo simulation. *Phys Med Biol.* 1995;40(6):963-78.

116. Sterling P., Laughlin S. 2015. Principles of Neural Design. Cambridge, MA; London: The MIT Press.

117. Vos JJ, BoumanMA. J. Contribution of the Retina to Entopic Scatter. *Opt Soc Am.* 1964; 54:95-100.

118. Wässle H. Parallel processing in the mammalian retina. *Nat Rev Neurosci*. 2004;5(10):747–757.

119. Werner J. S., Chalupa L. M. 2014. The New Visual Neurosciences. London: The MIT Press

120. Hoon M, Okawa H, Della Santina L, Wong R. Functional architecture of the retina: development and disease. *Prog Retin Eye Res.* 2014;42:44-84.

121. Harris, W. A. Cellular diversification in the vertebrate retina. *Curr. Opin. Genet. Dev.* 1997;**7**, 651-658.

122. Almeida, A. D., Boije, H., Chow, R. W., He, J., Tham, J., Suzuki, S. C. and Harris, W. A. Spectrum of Fates: a new approach to the study of the developing zebrafish retina. *Development*. 2014;141,1971-1980.

123. He, J., Zhang, G., Almeida, A. D., Cayouette, M., Simons, B. D. and Harris, W. A. How variable clones build an invariant retina. *Neuron.* 2012;75, 786-798.

124. Chow, R. W., Almeida, A. D., Randlett, O., Norden, C., Harris, W. A. Inhibitory neuron migration and IPL formation in the developing zebrafish retina. *Development.* 2015;142, 2665-2677.

125. Holt, C. E., Bertsch, T. W., Ellis, H. M. and Harris, W. A. Cellular determination in the xenopus retina is independent of lineage and birth date. *Neuron.* 1988;1,15-26.

126. Green, E. S., Stubbs, J. L. and Levine, E. M. Genetic rescue of cell number in a mouse model of microphthalmia: interactions between Chx10 and G1-phase cell cycle regulators. *Development.* 2003;130,539-552.

127. Kay, J. N., Roeser, T., Mumm, J. S., Godinho, L., Mrejeru, A., Wong, R. O., Baier, H. Transient requirement for ganglion cells during assembly of retinal synaptic layers. Development. 2004;131,1331-1342.

128. Randlett, O., Macdonald, R. B., Yoshimatsu, T., Almeida, A. D., Suzuki, S. C., Wong, R. O. and Harris, W. A. Cellular requirements for building a retinal neuropil. *Cell Rep.* 2013;3,282-290.

129. Huberman, A. D., Clandinin, T. R. and Baier, H. Molecular and cellular mechanisms of lamina-specific axon targeting. *Cold Spring Harb. Perspect. Biol.* 2010;2, a001743.

130. Johnson DA, Zhang J, Frase S, Wilson M, Rodriguez-Galindo C, Dyer MA. Neuronal differentiation and synaptogenesis in retinoblastoma. *Cancer Res*. 2007;67(6):2701–2711.

131. Wei, X., Zou, J., Takechi, M., Kawamura, S. and Li, L. Nok plays an essential role in maintaining the integrity of the outer nuclear layer in the zebrafish retina. *Exp. Eye Res.* 2006;83, 31-44.

132. Macosko EZ, Basu A, Satija R, Nemesh J, Shekhar K, Goldman M, Tirosh I, Bialas AR, Kamitaki N, Martersteck EM, Trombetta JJ, Weitz DA, Sanes JR, Shalek AK, Regev A, McCarroll SA. Highly Parallel Genome-wide Expression Profiling of Individual Cells Using Nanoliter Droplets. *Cell.* 2015;161(5):1202-1214.

133. Amini, R., Rocha-Martins, M., & Norden, C. Neuronal Migration and Lamination in the Vertebrate Retina. *Frontiers in neuroscience*. 2018;11,742.

134. Brackenbury R, Rutishauser U, Edelman GM. Distinct calcium-independent and calcium-dependent adhesion systems of chicken embryo cells. *Proc. Natl. Acad. Sci. U.S.A.* 1981;78(1):387–91

135. Halbleib JM, Nelson WJ. Cadherins in development: cell adhesion, sorting, and tissue morphogenesis. *Genes Dev*. 2006;20(23):3199–3214.

136. Gross, J. M., Perkins, B. D., Amsterdam, A., Egaña, A., Darland, T., Matsui, J. I., Sciascia, S., Hopkins, N., & Dowling, J. E. Identification of zebrafish insertional mutants with defects in visual system development and function. *Genetics*. 2005;170(1), 245–261.

137. Carrara N, Weaver M, Piedade WP, Vöcking O, Famulski JK. Temporal characterization of optic fissure basement membrane composition suggests nidogen may be an initial target of remodeling. *Dev Biol*. 2019;452(1):43–54.

138. Erdmann B, Kirsch FP, Rathjen FG, Moré MI. N-cadherin is essential for retinal lamination in the zebrafish. *Dev Dyn*. 2003;226(3):570–577.

139. Shimizu T, Yabe T, Muraoka O, et al. E-cadherin is required for gastrulation cell movements in zebrafish. *Mech Dev*. 2005;122(6):747–763.

140. Warga, R. M., & Kane, D. A. Probing Cadherin Interactions in Zebrafish with E- and N-Cadherin Missense Mutants. *Genetics*. 2018;210(4),1391–1409.

141. Pontoriero, G. F., Smith, A. N., Miller, L. A., Radice, G. L., West-Mays, J. A., & Lang, R. A. Co-operative roles for E-cadherin and N-cadherin during lens vesicle separation and lens epithelial cell survival. *Developmental biology*. 2009;326(2), 403–417.

142. Sherry G. Babb James A. 2004. E-cadherin regulates cell movements and tissue formation in early zebrafish embryos. Marrs.

143. Hatta K, Kimmel CB, Ho RK, Walker C. The cyclops mutation blocks specification of the floor plate of the zebrafish central nervous system. *Nature*. 1991;350(6316):339–341.

144. Malicki J, Jo H, Pujic Z. Zebrafish N-cadherin, encoded by the glass onion locus, plays an essential role in retinal patterning. *Dev Biol*. 2003;259(1):95–108.

145. McKay BS, Irving PE, Skumatz CM, Burke JM. Cell-cell adhesion molecules and the development of an epithelial phenotype in cultured human retinal pigment epithelial cells. *Exp Eye Res*. 1997;65(5):661–671.

146. Chow RL, Lang RA. Early eye development in vertebrates. *Annu Rev Cell Dev Biol*. 2001;17:255-96.

147. Schmitt EA, Dowling JE. Early eye morphogenesis in the zebrafish, Brachydanio rerio. *J Comp Neurol*. 1994;344(4):532–542.

148. Hyung N., et al. Systemic Diagnostic Testing in Patients With Apparently Isolated Uveal Coloboma. *American journal of ophthalmology*, 2013;156(6):1159-1168.e4.

149. Williamson KA, Fitz Patrick DR. The genetic architecture of microphthalmia, anophthalmia and coloboma. *Eur J Med Genet.* 2014; 57: 369–380.

150. Hocking JC, Famulski JK, Yoon KH, et al. Morphogenetic defects underlie Superior Coloboma, a newly identified closure disorder of the dorsal eye. *PLoS Genet*. 2018;14(3):e1007246.

151. Yamada S., Nelson W. J. Localized zones of Rho and Rac activates drives initiation and expansion of epithelia cell-cell adhesion. *J. Cell Biol.* 2007;178,517-527.

152. James A, Lee C, Williams AM, Angileri K, Lathrop KL, Gross JM. The hyaloid vasculature facilitates basement membrane breakdown during choroid fissure closure in the zebrafish eye. *Dev Biol*. 2016;419(2):262–272.

153. Li H, Tierney C, Wen L, Wu JY, Rao Y. A single morphogenetic field gives rise to two retina primordia under the influence of the prechordal plate. *Development.* 1997;124(3):603-15.

154. Fu X, Sun H, Klein WH, Mu X. Beta-catenin is essential for lamination but not neurogenesis in mouse retinal development. *Dev Biol*. 2006;299(2):424–437.

155. Monte Westerfield. 2020. The zebrafish book. A guide for the laboratory use of zebrafish Danio (Brachydanio) rerio homepage. ZFIN <https://zfin.org/zf_info/zfbook/cont.html> Accessed 13 Jun 2019.

156. M. Brand, M. Granato, C. Nüsslein-Volhard. Keeping and raising zebrafish C. Nüsslein-Volhard, R. Dahm. 2002. Zebrafish – A Practical Approach, Oxford University Press.

157. Westerfield M. 2007. The Zebrafish Book, 5th Edition; A guide for the laboratory use of zebrafish (Danio rerio). Eugene, University of Oregon Press. University of Oregon Press.

158. Hanovice NJ, McMains E, Gross JM. Using GAL4-Inducible Transgenics to Modulate Rho GTPase Activity in Zebrafish. *Methods Mol Biol*. 2018;1821:359–370.

159. Scheer N, Groth A, Hans S. An instructive function for Notch in promoting gliogenesis in the zebrafish retina. *Campos-Ortega JA. Development.* 2001;128(7):1099-107.

160. Uribe RA, Gross JM. Immunohistochemistry on cryosections from embryonic and adult zebrafish eyes. *Csh Protocols*. 2007:pdb.prot4779.

161. Alexandra D. Almeida, Henrik Boije, Renee W. Chow, Jie He, Jonathan Tham, Sachihiro C. Suzuki, William A. Harris. Spectrum of Fates: a new approach to the study of the developing zebrafish retina. *Development.* 2014 141: 1971-1980.

162. Steffen A, Ladwein M, Dimchev GA, et al. Rac function is crucial for cell migration but is not required for spreading and focal adhesion formation. *J Cell Sci*. 2013;126(Pt 20):4572–4588.

163. Pyrgaki, C., Trainor, P., Hadjantonakis, A. K., & Niswander, L. Dynamic imaging of mammalian neural tube closure. *Developmental biology*. 2010;344(2),941–947.

164. Stern, J., and Temple, S. Retinal pigment epithelial cell proliferation. *Experimental biology and medicine (Maywood, N.J.)*, 2015;*240*(8),1079–1086.

165. Haga RB, Ridley AJ. Rho GTPases: Regulation and roles in cancer cell biology. *Small GTPases*. 2016;7(4):207–221.

166. Etienne-Manneville S, Hall A. Rho GTPases in cell biology. *Nature.* 2002;12;420(6916):629-35.

167. Boureux A, Vignal E, Faure S, Fort P. Evolution of the Rho family of ras-like GTPases in eukaryotes. *Mol Biol Evol*. 2007;24(1):203–216.

168. Spaargaren, M., & Bos, J. L. Rab5 induces Rac-independent lamellipodia formation and cell migration. *Molecular biology of the cell*. 1999;10(10), 3239–3250.

169. Kurokawa, K., Itoh, R. E., Yoshizaki, H., Nakamura, Y. O., & Matsuda, M. Coactivation of Rac1 and Cdc42 at lamellipodia and membrane ruffles induced by epidermal growth factor. *Molecular biology of the cell*. 2004;*15*(3),1003–1010.

170. Logan SM, Benson MD. Medial epithelial seam cell migration during palatal fusion. *J Cell Physiol*. 2020;235(2):1417–1424.

171. *Shuler CF, Guo Y, Majumder A, Luo RY.* Molecular and morphologic changes during the epithelial-mesenchymal transformation of palatal shelf medial edge epithelium in vitro. *Int J Dev Biol.* 1991;35(4):463-72.

172. *Shuler CF, Halpern DE, Guo Y, Sank AC.* Medial edge epithelium fate traced by cell lineage analysis during epithelial-mesenchymal transformation in vivo. *Dev Biol.* 1992;154(2):318-30.

173. *Sun D, Vanderburg CR, Odierna GS, Hay ED.* TGFbeta3 promotes transformation of chicken palate medial edge epithelium to mesenchyme in vitro. *Development.* 1998;125(1):95-105.

174. *Kang P, Svoboda KK.* Epithelial-mesenchymal transformation during craniofacial development. *J Dent Res.* 2005;84(8):678-90.

175. *Nawshad A, Lagamba D, Polad A, Hay ED. T*ransforming growth factor-beta signaling during epithelial-mesenchymal transformation: implications for embryogenesis and tumor metastasis. *Cells Tissues Organs.* 2005;179(1-2):11-23.

176. *Yu W, Ruest LB, Svoboda KK. R*egulation of epithelial-mesenchymal transition in palatal fusion. *Exp Biol Med (Maywood).* 2009;234(5):483-91.

177. Cell death in normal development. *Glücksmann A. Arch Biol (Liege).* 1965;76(2):419-37.

178. Fadool, J. M., & Dowling, J. E. Zebrafish: a model system for the study of eye genetics. *Progress in retinal and eye research*. 2008;*27*(1), 89–110.

179. Gestri, G., Link, B. A., & Neuhauss, S. C. The visual system of zebrafish and its use to model human ocular diseases. *Developmental neurobiology*. 2012;*72*(3), 302–327.

180. Thakar, R. G., Cheng, Q., Patel, S., Chu, J., Nasir, M., Liepmann, D., Komvopoulos, K., & Li, S. Cell-shape regulation of smooth muscle cell proliferation. *Biophysical journal*. 2009;*96*(8), 3423–3432.

181. Baker J, Garrod D. Epithelial cells retain junctions during mitosis. *J Cell Sci*. 1993;104 (Pt 2):415–425.

182. Tamai H, Shinohara H, Miyata T, et al. Pax6 transcription factor is required for the interkinetic nuclear movement of neuroepithelial cells. *Genes Cells*. 2007;12(9):983–996.

183. Baye, L. M., & Link, B. A. Interkinetic nuclear migration and the selection of neurogenic cell divisions during vertebrate retinogenesis. *The Journal of neuroscience: the official journal of the Society for Neuroscience*. 2007;*27*(38), 10143–10152.

184. Carman CV, Sage PT, Sciuto TE, et al. Transcellular diapedesis is initiated by invasive podosomes. *Immunity*. 2007;26(6):784–797.

185. Paz, H., Pathak, N., & Yang, J. (2014). Invading one step at a time: the role of invadopodia in tumor metastasis. *Oncogene*. 2014;*33*(33),4193–4202.

186. Lohmer, L. L., Kelley, L. C., Hagedorn, E. J., & Sherwood, D. R. Invadopodia and basement membrane invasion in vivo. *Cell adhesion & migration*. 2014;*8*(3), 246–255.

187. Levay M, Krobert KA, Wittig K, et al. NSC23766, a widely used inhibitor of Rac1 activation, additionally acts as a competitive antagonist at muscarinic acetylcholine receptors. *J Pharmacol Exp Ther*. 2013;347(1):69–79.

188. Kimmel CB, Ballard WW, Kimmel SR, Ullmann B, Schilling TF. Stages of embryonic development of the zebrafish. *Dev Dyn*. 1995;203(3):253–310.

189. Deml, B., Kariminejad, A., Borujerdi, R. H., Muheisen, S., Reis, L. M., & Semina, E. V. Mutations in MAB21L2 result in ocular Coloboma, microcornea and cataracts. *PLoS genetics*. 2015;*11*(2),e1005002.

190. Deml B, Kariminejad A, Borujerdi RH, Muheisen S, Reis LM, Semina EV. Mutations in MAB21L2 result in ocular Coloboma, microcornea and cataracts. *PLoS Genet*. 2015;11(2):e1005002.

191. Small J. V., Celis J. E. Filament arrangements in negatively stained cultured cells: the organization of actin. *Eur. J. Cell Biol.* 1978;16:308–325.

192. Kwan KM, Fujimoto E, Grabher C, et al. The Tol2kit: a multisite gateway-based construction kit for Tol2 transposon transgenesis constructs. *Dev Dyn*. 2007;236(11):3088–3099.

193. Hatta K, Tsujii H, Omura T. Cell tracking using a photoconvertible fluorescent protein. *Nat Protoc*. 2006;1(2):960–967.

194. Richardson, R., Owen, N., Toms, M. et al. Transcriptome profiling of zebrafish optic fissure fusion. *Sci Rep* . 2019;9, 1541.

195. Placinta M, Shen MC, Achermann M, Karlstrom RO. A laser pointer driven microheater for precise local heating and conditional gene regulation in vivo. Microheater driven gene regulation in zebrafish. *BMC Dev Biol*. 2009;9:73.

196. Albertinazzi C, Cattelino A, de Curtis I. Rac GTPases localize at sites of actin reorganization during dynamic remodeling of the cytoskeleton of normal embryonic fibroblasts. *J Cell Sci*. 1999;112 (Pt 21):3821–3831

APPENDIX A

INSTITUTIONAL ANIMAL CARE AND USE COMMITTEE APPROVAL

IACUC Memorandum

To: Andrea James

From: Laura Martin, Director of Compliance and Operations

CC: IACUC Files

Date: 10/22/19

Re: IACUC Protocol 1912BC-AJ-F-21 Approval

The UNC IACUC has completed a final review of your protocol "Regulation of Adhesion during Choroid Fissure Closure in Zebrafish". The protocol review was based on the requirements of Government Principles for the Utilization and Care of Vertebrate Animals Used in Testing, Research, and Training; the Public Health Policy on Humane Care and Use of Laboratory Animals; and the USDA Animal Welfare Act and Regulations. Based on the review, the IACUC has determined that all review criteria have been adequately addressed. The PI/PD is approved to perform the experiments or procedures as described in the identified protocol as submitted to the Committee. This protocol has been assigned the following number 1912BC-AJ-F-21.

The next annual review will be due before October 22, 2020.

Sincerely,

Laura Martin, Director of Compliance and Operations